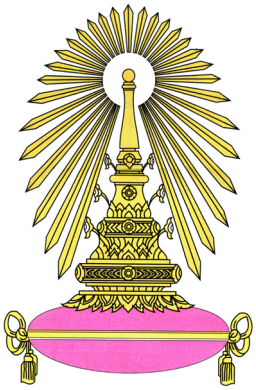



รายงานวิจัยฉบับสมบูรณ์

# โครงการ การพัฒนาวิธีการรักษามะเร็งท่อน้ำดีทางเลือกผ่านการกระตุ้นการตายแบบอะพอพโทซิสโดยโทลล์ไลค์รีเซฟเตอร์สามไลแกนและสารสะแมกไมมิติก

โดย อาจารย์ ดร. ศิริพร จิตแก้ว

2 เมษายน 2562

สัญญาเลขที่ MRG6080130

# รายงานวิจัยฉบับสมบูรณ์

# โครงการ การพัฒนาวิธีการรักษามะเร็งท่อน้ำดีทางเลือกผ่านการกระตุ้นการตายแบบอะพอพโทซิสโดยโทลล์ไลค์รีเซฟเตอร์สามไลแกนและสารสะแมกไมมิติก


| คณะผู้วิจัย | สังกัด |
|---|---|
| 1. อาจารย์ ดร.ศิริพร จิตแก้ว | จุฬาลงกรณ์มหาวิทยาลัย |
| 2. ศาสตราจารย์ ดร.นพ.อภิวัฒน์ มุทิรางกูร | จุฬาลงกรณ์มหาวิทยาลัย |
| 3. นายธัญพิสิษฐ์ ล้อมพิทักษ์ | จุฬาลงกรณ์มหาวิทยาลัย |



สนับสนุนโดยสำนักงานคณะกรรมการการอุดมศึกษา
และสำนักงานกองทุนสนับสนุนการวิจัย

# บทคัดย่อ

**รหัสโครงการ :** MRG6080130

**ชื่อโครงการ :** การพัฒนาวิธีการรักษามะเร็งท่อน้ำดีทางเลือกผ่านการกระตุ้นการตายแบบอะพอพโทซิสโดยโทลล์ไลค์รีเซฟเตอร์สามไลแกนและสารสะแมกไมมิติก

**ชื่อนักวิจัย :** อาจารย์ ดร. ศิริพร จิตแก้ว ศาสตราจารย์ ดร.นพ.อภิวัฒน์ มุทิรางกูร และนายธัญพิสิษฐ์ ล้อมพิทักษ์ จุฬาลงกรณ์มหาวิทยาลัย

**E-mail Address:** Siriporn.ji@chula.ac.th

**ระยะเวลาโครงการ :** 2 ปี

มะเร็งท่อน้ำดี เป็นมะเร็งที่มีอัตราการเสียชีวิตที่สูง และเป็นปัญหาสาธารณสุขที่สำคัญของประเทศไทย เนื่องจากยังขาดการรักษาที่มีประสิทธิภาพ ดังนั้นการพัฒนาวิธีการรักษาใหม่จึงเป็นสิ่งจำเป็นยิ่ง มะเร็งท่อน้ำดีมีความสัมพันธ์กับการอักเสบเรื้อรัง ดังนั้นอาจส่งผลให้เพิ่มการแสดงออกของโทลล์ไลค์รีเซฟเตอร์สาม โดยมีรายงานว่าโทลล์ไลค์รีเซฟเตอร์สามไลแกน หรือสารโพลีไอซี มีความสามารถในการเหนี่ยวนำให้เซลล์มะเร็งบางชนิดตายผ่านอะพอพโทซิส แต่อย่างไรก็ตามในมะเร็งที่มีการทำงานที่เพิ่มขึ้นของเอนเอฟแคปป้าบีจะส่งผลให้มีการเพิ่มการแสดงออกของโปรตีนซีไอเอพีหนึ่งและสอง และมายับยั้งการตายของเซลล์ที่ถูกกระตุ้นด้วยโทลล์ไลค์รีเซฟเตอร์สามไลแกน โปรตีนซีไอเอพีหนึ่งและสองสามารถสลายตัวได้ผ่านทางสารสะแมกไมมิติก เพื่อพัฒนาวิธีการรักษาแบบใหม่ในมะเร็งท่อน้ำดี คณะผู้วิจัยทำการรักษาร่วมโดยใช้โทลล์ไลค์รีเซฟเตอร์สามไลแกน และสารสะแมกไมมิติก การศึกษาการแสดงออกของโทลล์ไลค์รีเซฟเตอร์สามในชิ้นเนื้อของคนไข้มะเร็งท่อน้ำดี จำนวน 88 ราย พบว่ามีการแสดงออกที่เพิ่มสูงขึ้นในชิ้นเนื้อมะเร็งท่อน้ำดี เมื่อเปรียบเทียบกับบริเวณท่อน้ำดีปกติ ($p < 0.05$) การแสดงออกของโทลล์ไลค์รีเซฟเตอร์สามมีความจำเพาะกับเซลล์มะเร็งท่อน้ำดีเพาะเลี้ยง 6 ชนิด และไม่พบการแสดงออกในเซลล์ท่อน้ำดีเพาะเลี้ยงปกติ การศึกษาในเซลล์มะเร็งท่อน้ำดีเพาะเลี้ยง จำนวน 2 ชนิด พบว่าสารสะแมกไมมิติกเหนี่ยวนำให้มีการสลายตัวของโปรตีนซีไอเอพีหนึ่งและสอง และเสริมฤทธิ์กับโทลล์ไลค์รีเซฟเตอร์สามไลแกน ในการเหนี่ยวนำให้เซลล์มะเร็งท่อน้ำดีตายแบบอะพอพโทซิสโดยไม่ส่งผลต่อเซลล์ท่อน้ำดีเพาะเลี้ยงปกติ การตายแบบอะพอพโทซิสพบว่าเกิดผ่านทางการทำงานของเอนไซม์แคสเปสแปด การศึกษากลไกเพิ่มเติมโดยการยับยั้งการแสดงออกของโปรตีนไคเนสริฟหนึ่งโดยเทคโนโลยีคริสเปอร์แคสไนน์ พบว่าการตายของเซลล์เกิดผ่านทางการควบคุมของโปรตีนไคเนสริฟหนึ่ง กล่าวโดยสรุปงานวิจัยนี้ถือเป็นงานวิจัยแรกที่มีการค้นพบการเสริมฤทธิ์กันระหว่างสารสะแมกไมมิติกและโทลล์ไลค์รีเซฟเตอร์สามไลแกนในการเหนี่ยวนำให้เซลล์มะเร็งท่อน้ำดีตายผ่านทางอะพอพโทซิส และมีความสำคัญยิ่งเพื่อใช้เป็นแนวทางในการพัฒนาการรักษามะเร็งท่อน้ำดีแบบใหม่ที่มีประสิทธิภาพเพิ่มสูงขึ้น เพื่อเพิ่มอัตราการรอดชีวิตของผู้ป่วยมะเร็งท่อน้ำดี

**คำหลัก:** มะเร็งท่อน้ำดี, โทลล์ไลค์รีเซฟเตอร์สาม, สารสะแมกไมมิติก, อะพอพโทซิส, โปรตีนไคเนสริฟหนึ่ง

**Abstract**

**Project Code:** MRG6080130

**Project Title:** Combination treatment of Smac mimetic and TLR3 ligand-induced apoptosis as a novel therapeutic strategy for cholangiocarcinoma

**Investigator:** Dr. Siriporn Jitkaew, Prof. Dr. Apiwat Mutirangura, Mr. Thanpisit Lomphithak, Chulalongkorn University

**E-mail Address:** Siriporn.ji@chula.ac.th

**Project Period:** 2 years

Cholangiocarcinoma (CCA) has high mortality rate and becomes one of the major health problems in Thailand due to the lack of effective therapy, highlighting the need for new treatment strategies. CCA is associated with chronic inflammation that could upregulate Toll-like receptor 3 (TLR3) in CCA cells. TLR3 ligand or Poly(I:C), a promising adjuvant for cancer immunotherapy has been shown to directly induce apoptosis in selected cancers. However, in some types of cancer, there is dysregulation of NF-kB signaling pathway leading to the upregulation of cellular inhibitor of apoptosis proteins (cIAPs) 1 and 2. The upregulation of cIAP1 and cIAP2 has been shown to be a negative regulator of TLR3 ligand-induced apoptosis that can be removed by a small molecule antagonist of IAPs called Smac mimetic. This led us to ask the research question whether the combination treatment of TLR3 ligand and Smac mimetic could synergistically induce CCA apoptosis. Here, we investigated the expression of TLR3 in CCA surgical specimens obtained from 88 patients and in 6 CCA cell lines and an immortalized cholangiocyte. TLR3 expression was significantly higher in tumor tissues when compared to adjacent tumor tissues ($p < 0.05$), while TLR3 was specifically expressed in CCA cell lines, but not in an immortalized cholangiocyte. The combination treatment of TLR3 ligand or Poly(I:C) and Smac mimetic synergistically and specifically induced apoptosis in two representative CCA cell lines, but not in a non-tumor cholangiocyte. Apoptosis was activated through caspase-8-dependent pathway. In addition, we identified receptor-interacting protein kinase 1 (RIPK1) as a mediator of TLR3 ligand and Smac mimetic-induced apoptosis. This is the first study demonstrating that TLR3 ligand and Smac mimetic synergistically induced apoptosis in CCA cells with important implications for development a novel therapeutic strategy for CCA which could lead to increase survival rate of CCA patients.

**Keywords:** Cholangiocarcinoma, Toll-like receptor 3, Smac mimetic, Receptor-interacting protein kinase 1, Apoptosis

## Executive Summary

Cholangiocarcinoma (CCA) is predominantly found in Thailand and is one of the leading cause of death. To date, there are no effective therapies highlighting the need for new treatment strategies. Chronic inflammation has been generally considered to play important roles in the development of CCA following liver fluke, primary sclerosing cholangitis, and hepatitis viral infection which suggests the immune related etiology of CCA. Therefore, the upregulation of pattern recognition receptor in response to chronic inflammation such as Toll like receptor 3 (TLR3) in CCA cells was hypothesized and could be developed as a therapeutic target for CCA treatment. Dysregulated expression and activation of NF-KB proteins have been observed in CCA that may lead to the upregulation of cellular inhibitor of apoptosis protein 1 and 2 (cIAP1 and cIAP2), two of nuclear factor KB (NF-KB) target genes. cIAP1 and cIAP2 have been observed as a negative regulator of TLR3 ligands-induced apoptosis. In order to develop a novel treatment targeting TLR3-induced CCA apoptosis, we therefore screened for the expression of cIAP1, cIAP2 and TLR3 proteins in 6 different CCA lines including KKU100, KKU213, KKU214, RMCCA-1, KKU-M055 and HuCCT-1, while MMNK1, an immortalized cholangiocyte was used as a non-tumor or normal cholangiocyte control. We found high expression of cIAP1 in CCA cell lines and the expression of cIAP1 was similar in both 6 CCA cells and an immortalized cholangiocyte, while cIAP2 was differentially expressed in CCA cell lines and was slightly expressed in an immortalized cholangiocyte. In addition, the expression of TLR3 was only seen in all 6 CCA cell lines, but not in an immortalized cholangiocyte, MMNK1. To induce apoptosis in CCA cells, we transfected a synthetic analog of double-stranded RNAs, called Poly(I:C) which activate toll-like receptor 3 (TLR3) signaling and has been used as a potent adjuvant in cancer immunotherapy into CCA cells and an immortalized cholangiocyte. Poly(I:C) alone did not induce apoptosis in both CCA cells and an immortalized cholangiocyte, this is probably because of the presence of the negative regulators, cIAP1 and cIAP2 in these cells. We therefore removed cIAP1 and cIAP2 by using Smac mimetic, a small molecule antagonist of cIAP1 and cIAP2 which is currently entered clinical trials for treatment of some cancers. Interestingly, the combination treatment of Smac mimetic and Poly(I:C) markedly induced apoptosis in two representative CCA cell lines, but not in an immortalized cholangiocyte. The synergistic effect of the combination treatment was confirmed by combination index (CI index). TLR3 ligand and Smac mimetic-induced apoptosis was activated through caspase-8 dependent pathway. In addition, we identified receptor-interacting protein kinase 1 (RIPK1) as a mediator of TLR3 ligand and Smac mimetic-induced apoptosis which was confirmed by

a functional deletion of *RIPK1* gene by CRISPR/cas9 technology. In order to study the clinical relevance of TLR3 expression in CCA patients, we analyzed the expression of TLR3 in paraffin-embedded CCA primary tissues obtained from 88 CCA patients by Immunohistochemistry. TLR3 expression was mainly localized in the cytoplasm of CCA cells and was significantly higher expressed in tumor tissues when compared to adjacent tumor tissues ($p < 0.05$). This is the first study demonstrating that TLR3 ligand and Smac mimetic synergistically induced apoptosis in CCA cells with important implications for development a novel therapeutic strategy for CCA patients.

## วัตถุประสงค์

To develop a novel anti-cancer treatment for CCA, we examined the combination treatment of Smac mimetic and poly(I:C)-induced apoptosis in CCA cell lines.

**1.1** To examine the expression of cIAP1, cIAP2 and TLR3 proteins in CCA cell lines

**1.2** To examine the expression of TLR3 proteins in primary CCA tissues

**1.3** To induce the degradation of cIAP1 and cIAP2 by Smac mimetic

**1.4** To examine apoptosis induction by Smac mimetic or poly(I:C) or the combination of Smac mimetic and poly(I:C) treatment

**1.5** To determine the role of RIP1 as a mediator of Smac mimetic and poly(I:C)-induced apoptosis using CRISPR/cas9-mediated deletion of *RIP1* gene

## วิธีการทดลอง

**1. Human CCA cell lines as an *in vitro* model**

The expression of TLR3, cIAP1 and cIAP2 were examined in 6 different CCA cell lines including KKU100, KKU213, KKU214, KKU-M055, RMCCA-1, and HuCCT-1. MMNK1, an immortalized cholangiocyte was used as a non-tumor or normal cholangiocyte control. All cell lines were maintained in Ham's F12 medium containing 10% fetal bovine serum

(FBS) and 100 U/mL penicillin/100 μg/mL streptomycin (Pen/Strep). All cell lines will be maintained at 37 ºC in a 5% $CO_2$ humidified atmosphere.

**2. Detection of cIAP1, cIAP2 and TLR3 protein expression by western blot analysis**

We hypothesized that cIAP1 and cIAP2 are overexpressed in CCA cells and TLR3, one of pattern recognition receptors is expressed in CCA cells, therefore 6 different CCA cell lines and MMNK1 were recruited in this study in order to examine the expression of cIAP1, cIAP2, and TLR3. The cells were lysed in RIPA lysis buffer in the presence of protease cocktail inhibitor. Total protein (20-50 μg) were separated on a 10% denaturing polyacrylamide gel and transferred to a PVDF membrane. Membrane were probed with cIAP1, cIAP2, and TLR3 primary antibodies following by probing with horseradish peroxidase conjugated-secondary antibody. The membranes were developed using Enhanced Chemiluminescense system. Actin was used as a loading control. Each experiment was performed in three independent experiments. Two representative CCA cell lines that expressed TLR3 were chosen and used for the rest of experiments.

**3. Detection of TLR3 protein expression in CCA primary tissues by Immunohistochemical staining**

**3.1 Patient selection and clinical data collection**

Ten percent buffered formalin fixed and paraffin-embedded tissue specimens were retrieved from 88 CCA patients (Intrahepatic CCA = 21 samples and Hilar CCA = 67 samples) who underwent curative surgery at Tohoku University Hospital, Sendai, Japan between 2005 and 2015 in this study. Clinicopathological parameters of individual patient examined was summarized in Supplementary Table S1. The study protocol was approved by IRB of Tohoku University School of Medicine, Sendai, Japan.

### 3.2 Immunohistochemistry and evaluation

In all 88 CCA patients examined in this study, 3 μm sections were cut from formalin-fixed, paraffin-embedded tissue blocks and placed on clean glue coated glass slides. The sections were then de-paraffinized in xylene and re-hydrated in graded alcohol, and autoclaved for 5 min in an antigen retrieval solution to retrieve antigen epitopes. After antigen retrieval, the slides were blocked with 3% hydrogen peroxide at room temperature for 10 min. The slides were subsequently incubated with TLR3 antibody at 4°C for overnight. Subsequently, the slides were incubated with biotin-streptavidin horseradish peroxidase-conjugated anti-rabbit secondary antibody at room temperature for 1 h, after that the antigen-antibody complexes were visualized with 3,3'-diaminobenzidine tetrahydro-chloride solution and then counterstain with hematoxylin. Tissue sections of breast cancers were used as a positive control for TLR3 staining. For the negative controls, the primary antibodies were omitted in the procedure of immunostaining. Histopathological and immunohistochemical analysis were determined by 2 of the investigators using identical microscopes (BX50; Olympus, Tokyo, Japan). Evaluation of TLR3 immunoreactivity was carried out in a high-power field (×400). For semiquantitative analysis of immunoreactivity of the TLR3, the modified H-score was employed. The H-score was defined by >500 tumor cells count from 3 different representative fields, giving a possible range of 0–300. H-score was calculated from the formula (%Strong x 3) + (%Moderate x 2) +%Weak. If the H-score is 0-50, 51-100, 101-200, 201-300, it notes as TLR3 expression intensity negative, low, moderate and strong, respectively.

**4. cIAP1 and cIAP2 degradation by Smac mimetic**

In order to neutralize the anti-apoptotic activity of cIAP1 and cIAP2, a small molecule called Smac mimetic (SM-164) that targets cIAP1 and cIAP2 for proteasomal degradation was used in this study. SM-164 is a kind gift from Dr. Shaomeng Wang (University of Michigan, Ann Arbor, Michigan, USA). KKU100, KKU213, and MMNK1 were treated with SM-164 at concentration of 5 nM for 30 min, 1 h, 2 h, and 4 h. The cells were collected with RIPA lysis buffer and subjected to western analysis to detect cIAP1 and cIAP2 expression following SM-164 treatment. Actin was used as a loading control. Each experiment was performed in three independent experiments.

**5. Apoptosis induction and detection**

**5.1 Determination of cell viability by MTT assay and calculation of synergistic effect**

To preliminary screen for the sensitivity of Poly(I:C) and Smac mimetic-induced apoptosis, CCA cell lines were cultured in 96 well plates for overnight. The cells were treated with 2.5, 5, and 10 nM of SM-164 or 1, 2.5, 5, and 12.5 μg/ml Poly (I:C) for 24 h. For the combination treatment, the cells were pretreated with SM-164 for 2 h following by transfection of Poly(I:C) for 24 h. MTT assay was used to analyze cell viability. MTT assay or 3-(4,5-dimethylthiazol-2-yl)-2,5-diphenyltetrazolium bromide (MTT) assay is a colorimetric assay for measuring the cell metabolic activity due to NAD(P)H flux in the cell. Mitochondrial reductase reduces tetrazole (yellow) into formazan cystals (blue-purple) in the viable cell. The MTT solution was added to the culture medium to the final concentration of 0.25 mg/ml and the plate was incubated in 5% CO2 at 37 ºC for 2-3 hrs. Then, the culture medium was removed and 100 µl of DMSO was added to solubilize the formazan crystals. The absorbance of each sample was measured at 550 nm in microplate reader and was

calculated into the percentage of cell viability normalized to DMSO-treated control. In addition, combination index (CI) was calculated based on Chou-Talalay where CI = 1, CI < 1, and C > 1 indicates additive effect, synergism, and antagonism, respectively. To confirm apoptosis induction, specific markers of apoptosis were used.

**5.2 Determination of cell death by Annexin V/PI staining by flow cytometry**

Since MTT assay is unable to discriminate between an increase in cell death or a decrease in cell proliferation, the more specific marker of cell death was used to confirm the presence of cell death upon Poly(I:C) and Smac mimetic treatment. During the cells undergo apoptosis, phosphatidylserine (PS) which normally localizes in the inner leaflet of plasma membrane is externalized to the outer leaflet of plasma membrane and can be detected by recombinant protein Annexin V in the presence of calcium. In contrast to apoptotic cell death, when cells undergo necrosis, the plasma membrane is disrupted resulting in the cell impermeable dye, propidium iodide (PI) can enter the cells and binds to DNA. The cells were collected and stained with Annexin V-FITC and PI. The early apoptotic/necroptotic cells are positive for annexin V and negative for PI, while late apoptotic/necroptotic/necrotic cells are positive for both annexin V and PI staining. The dead cells were collected and quantitated by flow cytometry.

**5.3 Determination of caspase-8 and caspase-3 activation and PARP-1 cleavage by Western blot analysis**

In addition to Annexin V/PI staining, the caspase-8 and caspase-3 activation and Poly (ADP-Ribose) Polymerase 1 (PAPP-1), a substrate of caspase-3, cleavage were also determined. Following apoptosis treatment as previously described for 6 h, and 12 h, the cells were collected and lysed in RIPA lysis. Caspase-8 and caspase-3 activation and

PARP-1 cleavage were detected using specific antibodies using Western blot analysis. buffer.

**6. CRISPR/cas9-mediated deletion of *RIPK1* gene and Lentiviral production and induction**

In order to study the role of RIPK1 in TLR3 and caspase-8 signaling-mediated TLR3 and Smac mimetic-induced apoptosis in CCA cells, RIPK1 knock-out CCA cells were generated using CRISPR/cas9-mediated deletion of *RIPK1* gene. Lentiviral CRISPR plasmid targeting human *RIPK1* gene (NM_003804) has been generated previously from our laboratory at National Cancer Institute, National Institutes of Health, USA. The construction of CRISPR plasmid is according to Zhang's protocol. RIPK1 CRISPR plasmid was verified by DNA sequencing. The sequence of RIPK1 sgRNA was 5'-CACCGGATGCACGTGCTGAAAGCCG-3'. To generate lentiviral particles, HEK293T were co-transfected with packaging plasmid (pCMV-VSV-G) and envelope plasmid (pCMV-dr8.2-dvpr) and either CRISPR-V2 or CRISPR-RIPK1 plasmids. After 24 h, supernatants were collected and supernatants containing viral particles were filtered through a 0.45 μM sterile filter membrane. The lentiviral preparation was then used to infect the cells with 8 μg/mL of polybrene. After 24 h of infection, cells were selected with puromycin for a further 48 h. The deletion of *RIPK1* gene were confirmed by examining the functional expression of RIPK1 protein by Western blot analysis using a RIPK1 specific antibody. The CRISPR RIPK1 knock-out cells were used for further studies.

**7. Statistics and data analysis**

All experiments were carried out in three independent experiments. The results were expressed as mean ± S.D. Independent student's *t* test were used to evaluate the

statistical significance, and differences between mean values were considered significant when *p*-value is less than 0.05 ($p < 0.05$).

**ผลการทดลอง**

**1. The expression of cIAP1, cIAP2 and TLR3 proteins by Western blot analysis**

Chronic inflammation has been generally considered to play important roles in the development of CCA following liver fluke and primary sclerosing cholangitis, which suggests the immune related etiology of CCA. Therefore, the upregulation of pattern recognition receptor in response to chronic inflammation such as Toll like receptor 3 (TLR3) in CCA cells was hypothesized and could be used as a therapeutic target for CCA treatment. Dysregulated expression and activation of NF-KB proteins have been observed in CCA that may lead to the upregulation of cellular inhibitor of apoptosis protein 1 and 2 (cIAP1 and cIAP2), two of nuclear factor KB (NF-KB) target genes. cIAP1 and cIAP2 have been observed as a negative regulator of TLR3 ligands-induced apoptosis. In order to develop a novel treatment targeting TLR3-induced CCA apoptosis, we therefore screened for the expression of cIAP1, cIAP2 and TLR3 proteins in 6 different CCA lines including KKU100, KKU213, KKU214, RMCCA-1, KKU-M055 and HuCCT-1, while MMNK1, an immortalized cholangiocyte was used as a non-tumor or normal cholangiocyte control. The expression of cIAP1, cIAP2 and TLR3 proteins was examined by Western blot analysis. As we can see in figure 1 (cIAP1 and cIAP2) and figure 2 (TLR3), the expression of cIAP1 was similar between an immortalized cholangiocyte and 6 CCA cell lines, while the expression of cIAP2 was differentially expressed in all cell lines tested. Interestingly, TLR3 was only expressed in CCA cell lines, but not in an immortalized cholangiocytes. KKU100 and HuCCT-1 exhibit a strong TLR3 expression compared to a positive control, human transformed keratinocyte

HaCaT cells. In addition, RIPK1 expression, a proposed mediator of TLR3-induced apoptosis was also examined, the expression of RIPK1 was similar in all cell lines tested.

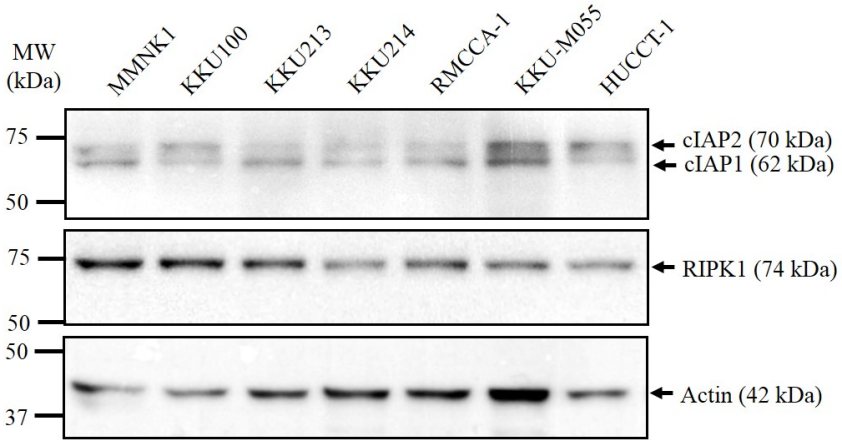


**Figure 1** The expression of cIAP1, cIAP2 and RIPK1 in CCA cell lines and an immortalized cholangiocyte, MMNK1. Actin was used as a loading control.

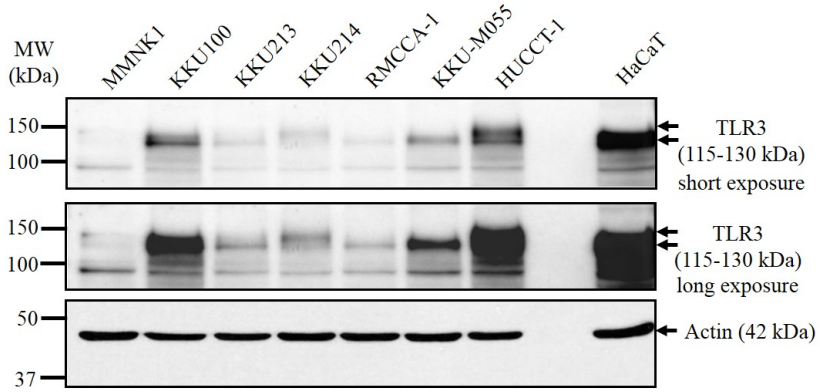


**Figure 2** The expression of TLR3 in CCA cell lines and an immortalized cholangiocyte, MMNK1. Actin was used as a loading control.

**2. A pilot study: the sensitivity of CCA cell lines and MMNK1 to Smac mimetic, Poly(I:C), and the combination of Smac mimetic and Poly(I:C) treatment by MTT assay**

Since CCA cell lines express TLR3, in order to examine whether the stimulation of TLR3 using synthetic analogs of double stranded RNAs (i.e. Poly(I:C) which activate TLR3

signaling could induce apoptotic cell death, a pilot study by using a single dose of Poly(I:C) and Smac mimetic that have been used widely were chosen. Since TLR3 is mostly expressed in endosome membrane, 2.5 μg/ml of Poly(I:C) (P) was transfected into CCA cells and MMNK1, 10 nM smac mimetic (S) was added directly into culture medium. The cells were treated alone with P or S or the combination of P and S for 24 h. Treatment with TNF-α and S was used as a positive comparison control. Cell viability was determined using MTT assay. As we can see from figure 3, KKU100 and KKU213 seem to be response to the combination of P and S treatment when compared to other CCA cell lines. RMCCA-1 and KKU-M055 were not sensitive to P and S treatment, but they were sensitive to TNF-α and S treatment, while KKU214 and HuCCT-1 were not sensitive to both P and S or TNF-α and S treatment. Interestingly, MMNK1, an immortalized cholangiocyte control was not sensitive to P and S treatment, but they were sensitive to TNF-α and S treatment, this result is consistent with no TLR3 expression in MMNK1. These results suggest that TLR3-induced cell death is specific to CCA cells, but not an immortalized cholangiocytes. Therefore, KKU100, KKU213 and MMNK1 as a non-tumor or normal cholangiocyte control were chosen as representative cell lines for further treatment optimization and analysis.

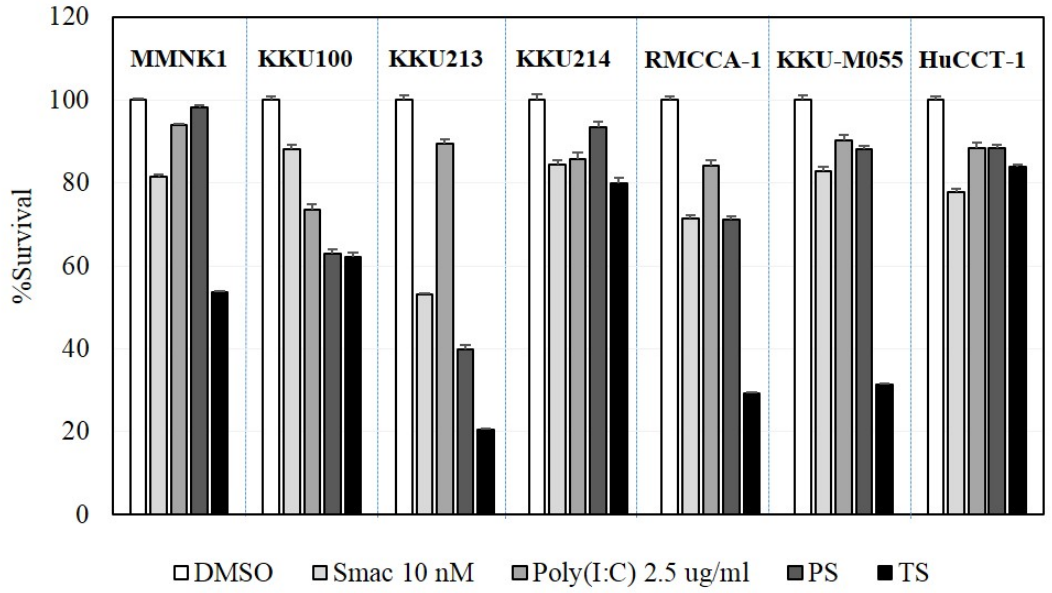


**Figure 3:** Cell viability after treatment with 2.5 µg/ml of Poly(I:C) (P), 10 nM Smac mimetic (S), P+S and TNF-α (T)+S for 24 h in CCA cell lines and MMNK1, a non-tumor or normal cholangiocyte control. Cell viability was determined using MTT assay.

### 3. Optimization of Smac mimetic-induced cIAP1 and cIAP2 degradation

Smac mimetic neutralizes the anti-apoptotic activity of cIAP1 and cIAP2 by targeting cIAP1 and cIAP2 for proteasomal degradation, in order to find an optimal time for Smac mimetic treatment, MMNK1, KKU100, and KKU213 were treated with Smac mimetic for 0.5, 1, and 2 h. After that, the expression of cIAP1 and cIAP2 was examined by Western blot analysis. As we can see in figure 4, cIAP1 and cIAP2 were gradually decreased after 1 h treatment and almost completely absent after 2 h treatment. Therefore, the cells were pre-treated with Smac mimetic for 2 h before adding Poly(I:C) or TNF-α for further experiments.

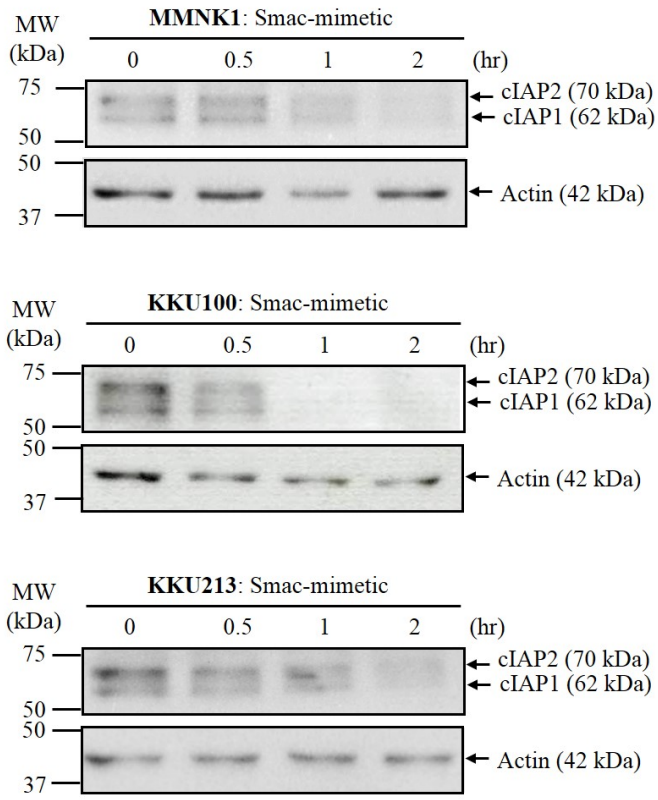


**Figure 4** The expression of cIAP1 and cIAP2 in KKU100, KKU213 and an immortalized cholangiocyte, MMNK1 after Smac mimetic treatment as indicated. Actin was used as a loading control.

**4. Optimization of Poly(I:C) and Smac mimetic-induced cell death and calculation of synergistic combination index (CI) in KKU100, KKU213 and an immortalized cholangiocyte, MMNK1**

Since KKU100 and KKU213 are two out of six CCA cell lines that seem to response well with the combination of Poly(I:C) and Smac mimetic, these two CCA cell lines were chosen for further optimization experiments to find the optimal dose of Poly(I:C) and Smac mimetic-induced CCA cell death. Cell death was determined using MTT assay. The synergistic effect of Poly(I:C) and Smac mimetic was calculated using CalcuSyn software and interpret as combination index (CI index) where CI < 0.9 = synergism, CI = 0.9-1.1 = additivity and CI > 1.1 = antagonism. The concentration of Poly(I:C) was varied from 1, 2.5,

5, 12.5 µg/ml, while the concentration of Smac mimetic was varied from 1, 5, 10, 25, and 50 nM depend on cell lines used. The cells were treated with either Poly(I:C) or Smac mimetic alone or the combination treatment, TNF-α and Smac mimetic treatment was included as a positive control. As we can see from figure 5, with CI index, the optimal dose of Poly(I:C) and Smac mimetic in KKU100 is at Poly(I:C) 2.5 µg/ml and Smac mimetic 50 nM, while the optimal dose of Poly(I:C) and Smac mimetic in KKU213 is at Poly(I:C) 2.5 µg/ml and Smac mimetic 5 nM.

A.

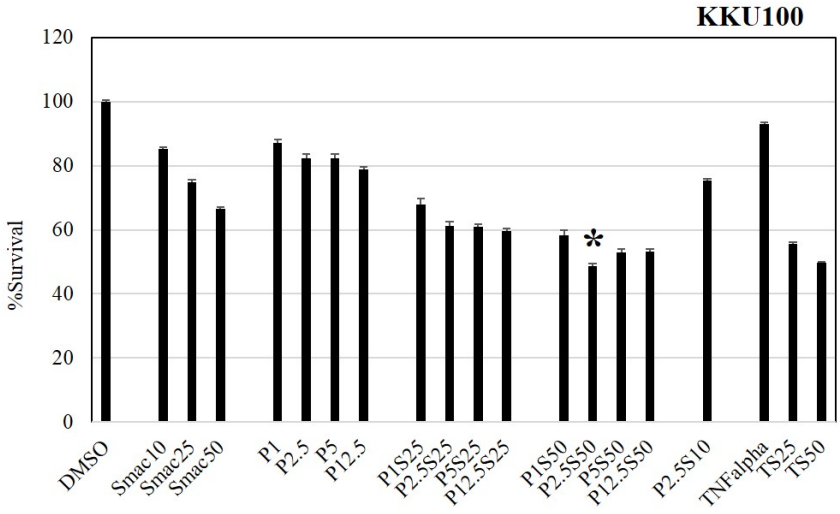


| KKU100 | | CI index | | |
|---|---|---|---|---|
| Smac (nM) | | 10 | 25 | 50 |
| Poly(I:C) (µg/ml) | 1 | ND | 0.58 | 0.61 |
| | 2.5 | 0.53 | 0.38 | 0.34 |
| | 5 | ND | 0.39 | 0.45 |
| | 12.5 | ND | 0.41 | 0.47 |

B.

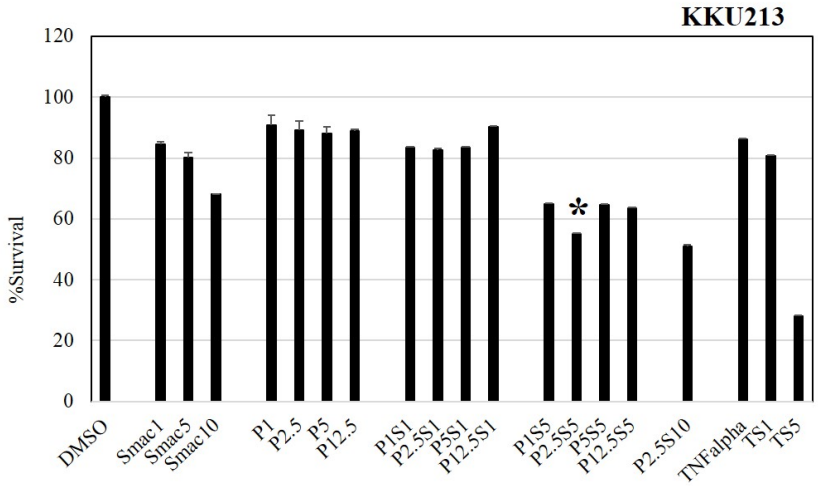


| KKU213 | | CI index | | |
|---|---|---|---|---|
| Smac (nM) | | 1 | 5 | 10 |
| Poly(I:C) (µg/ml) | 1 | 0.64 | 0.20 | ND |
| | 2.5 | 0.56 | 0.07 | 0.49 |
| | 5 | 0.65 | 0.19 | ND |
| | 12.5 | 1.14 | 0.17 | ND |

C.

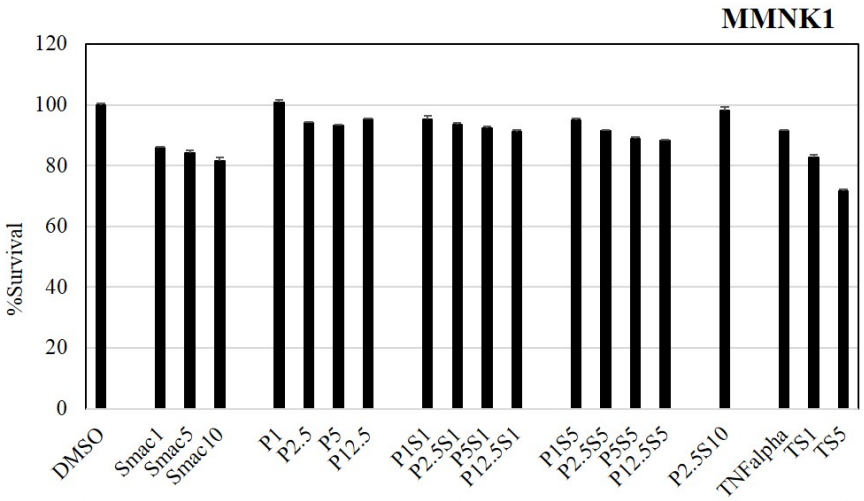


| MMNK1 | | CI index | | |
|---|---|---|---|---|
| Smac (nM) | | 1 | 5 | 10 |
| Poly(I:C) (µg/ml) | 1 | 4081.84 | 9081.82 | ND |
| | 2.5 | 138.09 | 95.20 | 57277.40 |
| | 5 | 50.41 | 16.44 | ND |
| | 12.5 | 16.17 | 12.25 | ND |

D.

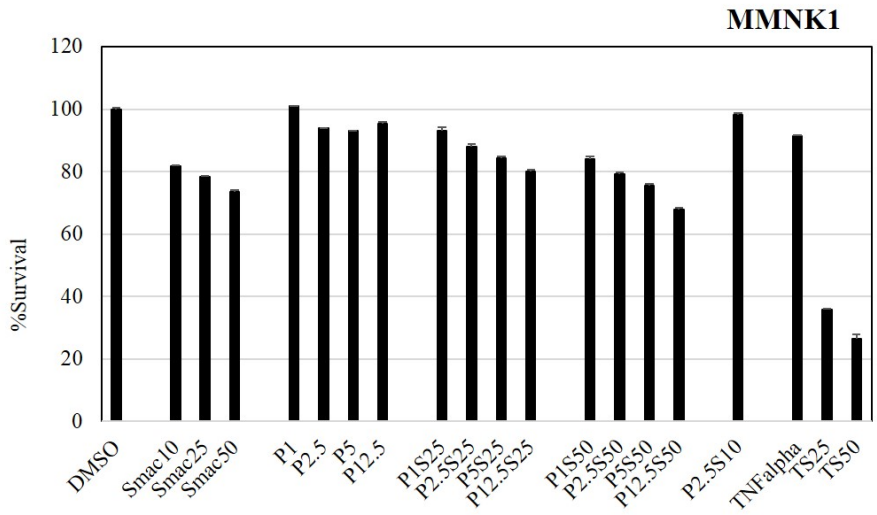


| MNNK1 | | CI index | | |
|---|---|---|---|---|
| Smac (nM) | | 10 | 25 | 50 |
| Poly(I:C) (µg/ml) | 1 | ND | 2669.09 | 17.11 |
| | 2.5 | 57277.40 | 52.14 | 3.13 |
| | 5 | ND | 9.16 | 1.18 |
| | 12.5 | ND | 2.29 | 0.61 |

**Figure 5** Cell viability after treatment with different concentrations of Poly(I:C) (P), or Smac mimetic (S) alone, or the combination treatment (P+S) and TNF-α (T)+S for 24 h in (A) KKU100, (B) KKU213, (C) MMNK1 with low dose of Smac mimetic and (D) high dose of Smac mimetic. Cell viability was determined using MTT assay and the synergistic effect was calculated and represented as CI index.

**5. Determination of Poly(I:C) and Smac mimetic-induced apoptosis in KKU100, KKU213 and an immortalized cholangiocyte, MMNK1**

In order to confirm apoptosis induction, specific markers of apoptosis were determined including by Annexin V and PI stating with or without pan-caspase inhibitor (zVAD-fmk) analyzed by flow cytometer and the activation of caspase-3, caspase-8 and PARP-1 cleavage by Western blot analysis.

**5.1 Determination of apoptosis by Annexin V and PI staining with or without pan-caspase inhibitor (zVAD-fmk)**

Following apoptosis treatment as previously described, MMNK1, KKU100, and KKU213 cells were collected and stained with Annexin V-FITC and PI. After that cell death was measured by flow cytometer. Annexin V positive and/or PI positive population were included as percentage (%) of cell death. As we can see in figure 6, MNNK1 cells were resistant to PS treatment, while they were still sensitive to TS treatment and cell death was completely inhibited by pan-caspase inhibitor (zVAD-fmk), suggesting that TS-induced apoptosis in MMNK1 cells. KKU100 cells were sensitive to PS and TS treatment and zVAD-fmk almost completely inhibited PS- and TS-induced cell death suggesting that both PS and TS specifically induced apoptosis in this cell. In contrast to KKU100, another representative CCA cell line, KKU213, both PS and TS induced cell death in this cell line, however zVAD-fmk partially inhibited PS- and TS-induced cell death, this probably because of the expression of protein called receptor interacting protein kinase-3 (RIPK3) in this cell (data not shown), the remaining cell death might switch to another cell death pathway called necroptosis, a novel regulated form of necrosis.

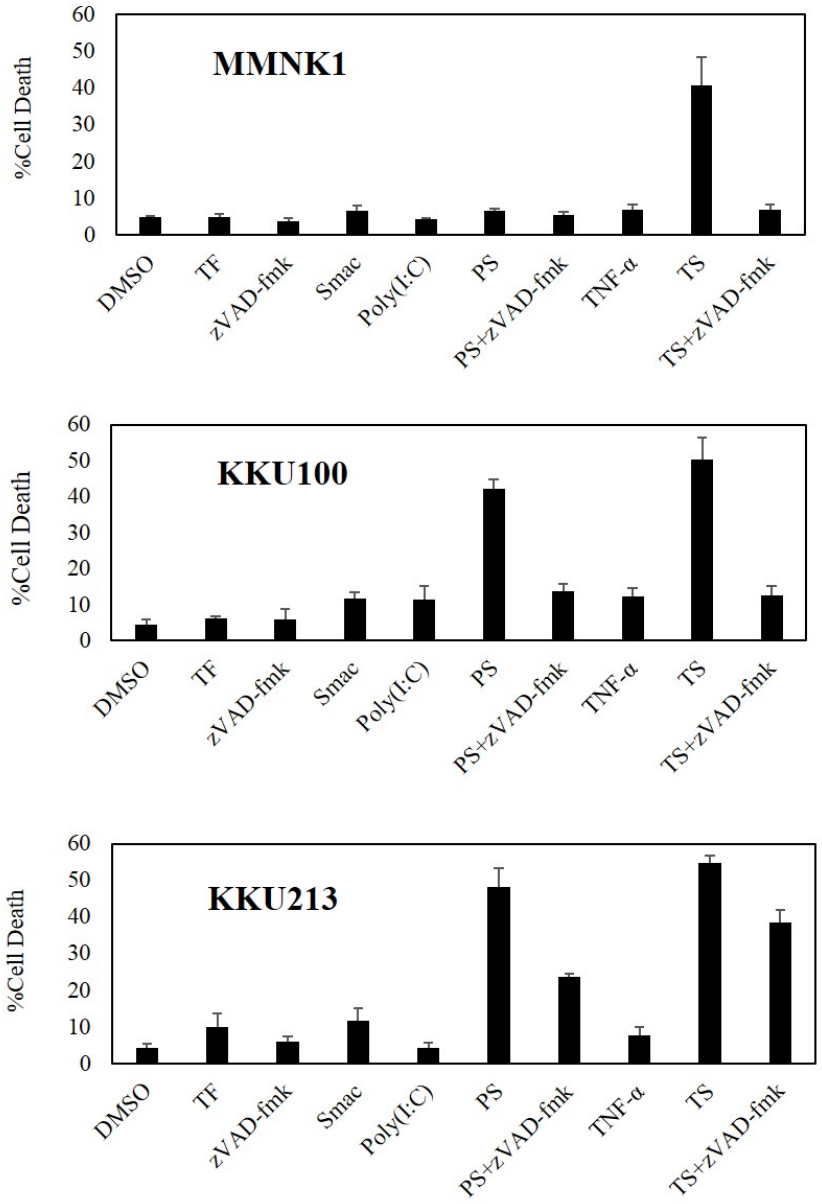


**Figure 6** Cell death after treatment with 2.5 μg/ml Poly(I:C) (P), or Smac mimetic (S) in KKU100 (50 nM), KKU213 (5 nM), and MMNK1 (5 nM) alone, or the combination treatment (P+S) and TNF-α (T)+S for 24 h. Cell death was determined by Annexin V/PI staining and analyzed by flow cytometer.

### 5.2 Determination of apoptosis by the activation of caspase-3, caspase-8 and PARP-1 cleavage by Western blot analysis

To further examine whether PS specifically induced apoptosis in CCA cells, more specific markers of apoptosis were examined. Since it has been demonstrated previously in

other cancer cells that Poly(I:C) induced apoptosis through extrinsic apoptosis pathway, therefore caspase-8, an initiator caspase for extrinsic pathway activation was examined. In addition, caspase-3, an executioner caspase activation as well as its substrate cleavage, PARP-1 was also examined by Western blot analysis. As we can see in figure 7, PS induced caspase-8 and caspase-3 activation as well as PARP-1 cleavage in both KKU100 and KKU213 cells.

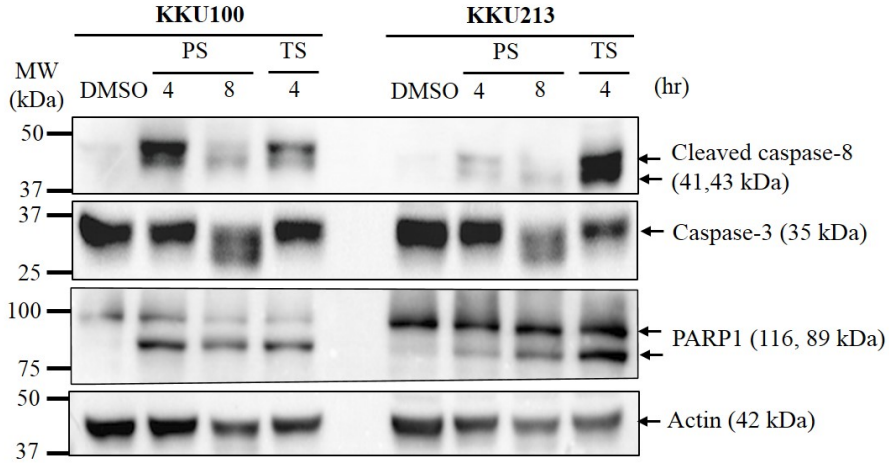


**Figure 7** Caspase-8, caspase-3 activation and PARP-1 cleavage. After the combination treatment of 2.5 μg/ml Poly(I:C) (P) and Smac-mimetic (S) in KKU100 (50 nM) and KKU213 (5 nM) for 4 and 8 h, or the combination treatment TNF-α (T)+S for 4 h as a positive control, cells were collected and subjected to Western blot analysis.

**6. Investigation the underlying mechanism of Poly(I:C) and Smac mimetic-induced apoptosis**

TLR3 and Smac mimetic treatment-induced apoptosis has been proposed to be mediated through caspase-8 and receptor interacting protein kinase 1 (RIPK1) dependent-signaling. In order to study the involvement of RIPK1 in this pathway, RIPK1 knock-out CCA cells were generated using CRISPR/cas9-mediated deletion of *RIPK1* gene.

### 6.1 Generation of RIPK1 knockout cells in KKU100 and KKU213

To generate lentiviral particles, HEK293T were co-transfected with packaging plasmid (pCMV-VSV-G) and envelope plasmid (pCMV-dr8.2-dvpr) and either CRISPR-V2 or CRISPR-RIPK1 plasmids. After 24 h, supernatants were collected and supernatants containing viral particles were filtered through a 0.45 μM sterile filter membrane. The lentiviral preparation was then used to infect the cells with 8 μg/mL of polybrene. After 24 h of infection, cells were selected with puromycin for a further 48 h. The deletion of *RIPK1* gene were confirmed by examining the functional expression of RIPK1 protein by Western blot analysis using a RIPK1 specific antibody. As we can see in figure 8, the expression of RIPK1 was absent in both KKU100 and KKU213 CRISPR RIPK1 knock out cells. Therefore, the CRISPR RIPK1 knock-out cells were used for further studies.

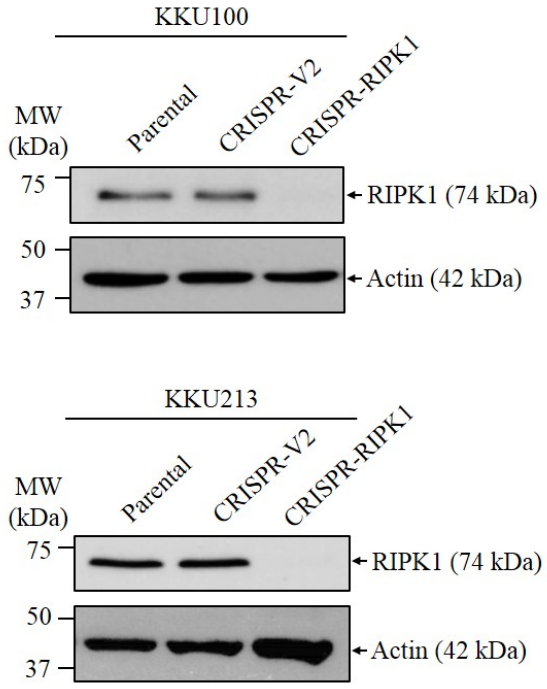


**Figure 8** The expression of RIPK1 in KKU100 and KKU213 knock-out cells. KKU100 and KKU213 were infected with CRISPR-V2 or CRISPR-RIPK1. The expression of RIPK1 was determined by Western blot analysis. β-actin served as loading control.

### 6.2 Determination of Poly(I:C) and Smac mimetic-induced apoptosis in RIPK1 knockout cells

In order to determine the sensitivity of Poly(I:C) and Smac-mimetic-induced apoptosis in KKU100 and KKU213 RIPK1 knock-out cells, CRISPR-V2 and CRISPR-RIPK1 KKU100 and KKU213 cells were treated with 2.5 μg/ml Poly(I:C) (P) and 50 nM (KKU100), 5 nM (KKU213) Smac mimetic (S) for 24 h, TNF-α and Smac mimetic were used as a comparative positive control. After 24 h, cells were collected and stained with Annexin V-FITC and PI followed by analysis of cell death by flow cytometry. As we can see in figure 9, the cell death in CRISPR-RIPK1 in both KKU100 and KKU213 was significantly lower when compared to CRISPR-V2 cells. The result was similar when RIPK1 knock-out KKU100 and KKU213 cells was treated with TNF-α and Smac mimetic which has previously been shown that TNF-α and Smac mimetic-induced RIPK1 dependent apoptosis. This result suggest that RIPK1 is required for Poly(I:C) and Smac-mimetic-induced apoptosis in KKU100 and KKU213.

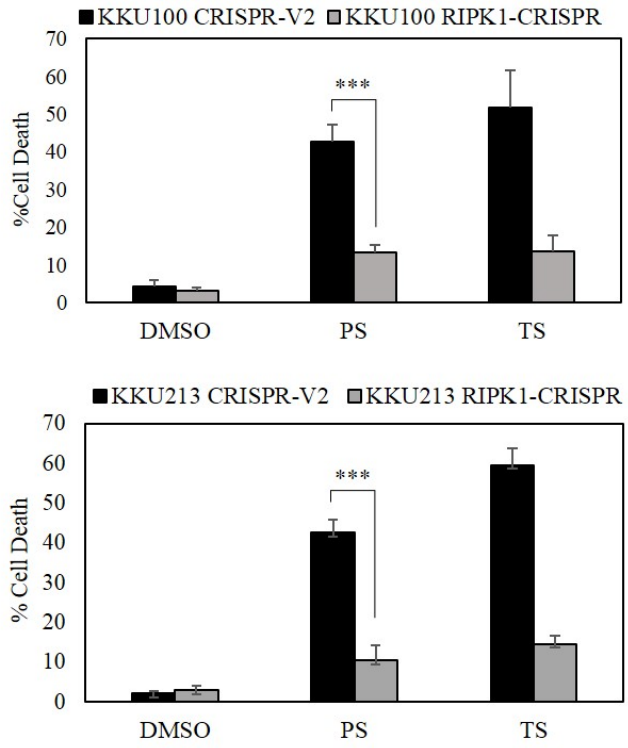


**Figure 9** Cell death after treatment with 2.5 µg/ml Poly(I:C) (P) and Smac mimetic (S) for 24 h in KKU100 and KKU213 RIPK1 knock-out cells. Cell death was determined by Annexin V/PI staining and analyzed by flow cytometer. Data presented as mean ± S.D. of three independent experiments are shown; * $p < 0.05$, ** $p < 0.01$, *** $p < 0.001$

## 7. Investigation of TLR3 expression in human CCA primary tissues

### 7.1 Optimization of TLR3 antibody for Immunohistochemistry of paraffin-embedded primary tissues

Since TLR3 seems to be differentially expressed in CCA cell lines, we then attempted to study the *in vivo* relevance of TLR3 expression in clinical cases of CCA. TLR3 was therefore immunostained by Immunohistochemistry in human CCA primary tissues. To verify and optimize for TLR3 antibody used for Immunohistochemistry, breast cancer tissues were used as positive staining. As we can see in figure 10, TLR3 was

positively staining in the cytoplasm of breast cancer tissues, while when 2nd antibody was omitted there was negatively staining (data not shown).

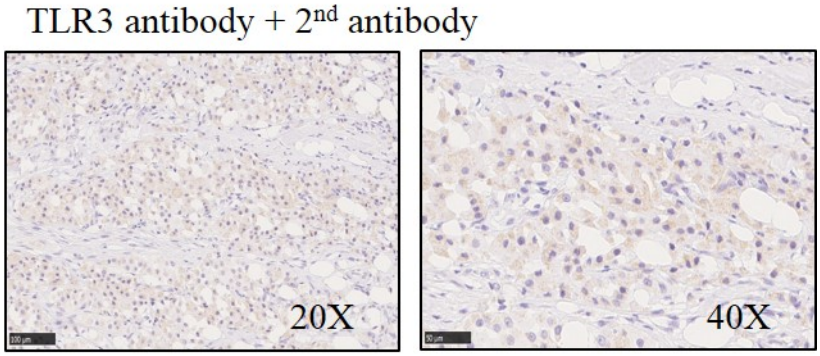


**Figure 10** Optimization of TLR3 Immunohistochemistry in breast cancer tissues. Breast cancer tissues were stained with TLR3 antibody (anti-TLR3 antibody [40C1285], ab13915, Abcam, Cambridge, UK, dilution 1:500)

**7.2 TLR3 expression in human CCA primary tissues**

In order to investigate the expression of TLR3 in CCA primary tissues, 10% buffered formalin fixed and paraffin-embedded tissue specimens were retrieved from 88 CCA patients (Intrahepatic CCA = 21 samples and Hilar CCA = 67 samples) who underwent curative surgery at Tohoku University Hospital, Sendai, Japan between 2005 and 2015 in this study. As we can see in figure 11 and 12, TLR3 immunoreacivity was differentially present and mainly localized in the cytoplasm of CCA tissues and normal cholangiocyte adjacent to tumor tissues.

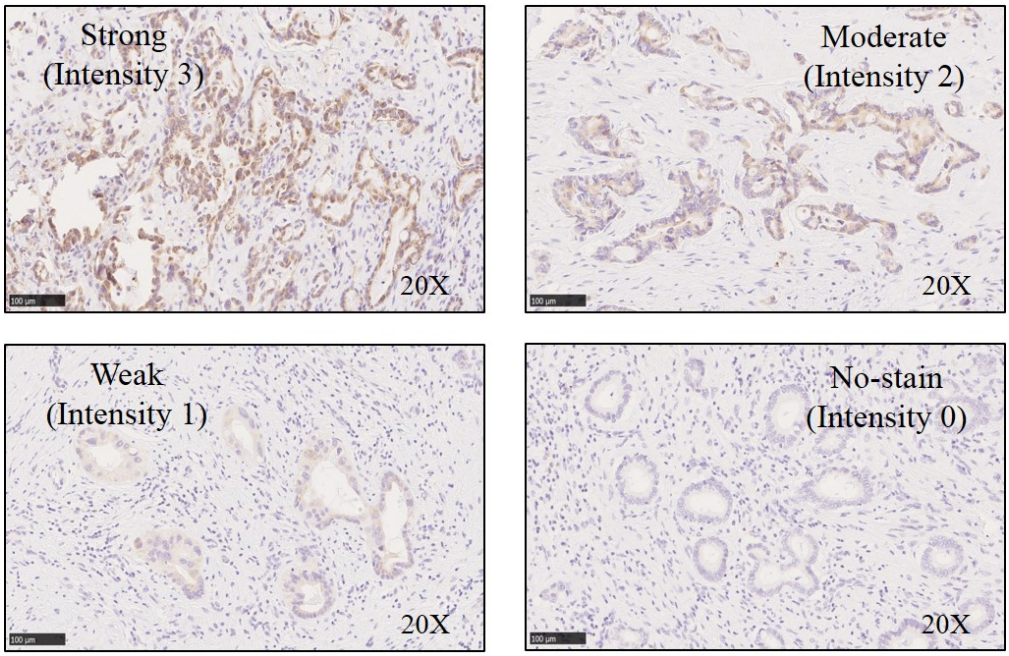


**Figure 11** Representative of H-score evaluation of TLR3 staining in CCA primary tissues

In addition, we further showed that TLR3 was expressed higher in tumor area compared to normal cholangiocyte adjacent to tumor tissues (All CCA, *p* value < 2.25E-7, Hilar CCA, *p* value < 2.84 E-7, Intrahepatic CCA *p* value = 0.69) (figure 12 and 13). In order to classified the expression level of TLR3 into subgroups, the H-score of TLR3 expression was tentatively classified as negative (0-50), low (51-100), moderate (101-200) and strong (201-300) and the percentages of each groups were summarized in figure 14. As we can see that the expression of TLR3 in CCA tissues was differentially expressed ranging from negative to high expression, while there was negative staining and most of patients was in low expression in normal cholangiocytes adjacent to tumor tissues.

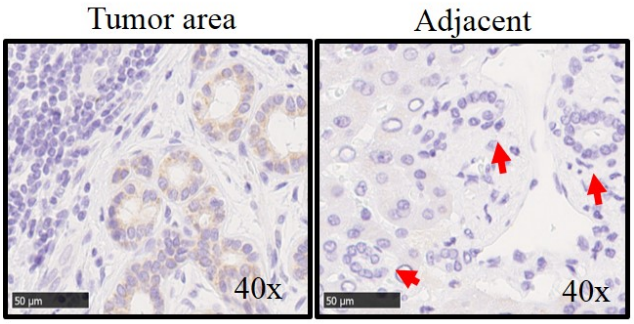


**Figure 12** Representative of TLR3 staining in CCA primary tissues, normal cholangiocyte adjacent to tumor tissues. Red arrowheads indicate bile ducts.

| Median of H-score | | n | Area | | *p*-value |
|---|---|---|---|---|---|
| | | | Tumor area | Tumor adjacent normal area | |
| TLR3 | All CCA | 88 | 78.0862 | 38.1818 | 2.2485E-7 |
| | Hilar CCA | 67 | 86.4925 | 36.2687 | 2.837E-9 |
| | Intrahepatic CCA | 21 | 51.1905 | 44.2857 | 0.689353 |

**Figure 13** Summarization of TLR3 staining in CCA primary tissues, normal cholangiocyte adjacent to tumor tissues

| All CCA | CCA | | Adjacent | |
|---|---|---|---|---|
| | % | n | % | n |
| Negative | 9.1 | 8 | 2.3 | 2 |
| Low | 63.7 | 56 | 97.7 | 86 |
| Moderate | 22.7 | 20 | 0 | 0 |
| Strong | 4.5 | 4 | 0 | 0 |

| Hilar CCA | CCA | | Adjacent | |
|---|---|---|---|---|
| | % | n | % | n |
| Negative | 4.5 | 3 | 3 | 2 |
| Low | 67.1 | 45 | 97 | 65 |
| Moderate | 23.9 | 16 | 0 | 0 |
| Strong | 4.5 | 3 | 0 | 0 |

| Intrahepatic CCA | CCA | | Adjacent | |
|---|---|---|---|---|
| | % | n | % | n |
| Negative | 23.8 | 5 | 0 | 0 |
| Low | 52.4 | 11 | 100 | 21 |
| Moderate | 19 | 4 | 0 | 0 |
| Strong | 4.8 | 1 | 0 | 0 |

**Figure 14** Summarization of TLR3 staining as evaluated by percent negative/positive staining. The H-score of TLR3 expression was tentatively classified as negative (0-50), low (51-100), moderate (101-200) and strong (201-300) and the percentages of each groups were summarized.

## สรุปและวิจารณ์ผลการทดลอง

CCA has high mortality rate due to the lack of effective therapy. In this study, we demonstrated for the first time that the combination treatment of Smac mimetic, an IAPs antagonist and TLR3 ligand or Poly(I:C)-induced caspase-8-dependent CCA apoptosis through RIPK1-dependent manner. TLR3 ligand or Poly(I:C) and Smac mimetic-induced apoptosis was specific to CCA cells, but did not affect non-tumor cholangiocyte which suggests that this treatment has less side effect to the surrounding normal tissues. This study has important clinical implication that could possibly be further developed as a novel therapeutic strategy for CCA patients.

We further investigated the clinical relevance of TLR3 expression which represents one of key molecules in the current therapeutic concept, TLR3 was significantly higher expressed in CCA primary tissues than adjacent tumor tissues. This result is consistent with the expression of TLR3 in CCA cell lines in which we observed that TLR3 did not expressed in non-tumor cholangiocyte, while TLR3 was differentially expressed in all CCA cell lines tested. Although in some CCA patients expressed low level of TLR3, we found that treatment with TLR3 ligand or Poly(I:C) strongly induced the expression of TLR3.

Although the results of this study has opened a novel therapeutic concept for CCA, this work is still in an early phase which requires further studies before it could be used in clinics. As all of the experiments conducted in this study were *in vitro* studies, therefore a few experiments needed to be done in animal model 1) testing the ability of Poly(I:C) and Smac mimetic to inhibit tumor growth *in vivo*. 2) the toxicity of this treatment in animal model and 3) the delivery of Poly(I:C) which is a dsRNA analog into tumor site. In addition, since both Poly(I:C) and Smac mimetic have been shown to contribute to anti-tumor

immunity, the ability of Poly(I:C) and Smac mimetic combination treatment to induce immunogenic cell death (ICD) and anti-tumor immunity is of interest to further increase the efficacy of the treatment.

**Output จากโครงการวิจัยที่ได้รับทุนจาก สกว.**

**1. ผลงานตีพิมพ์และอยู่ในระหว่างรอตีพิมพ์ในวารสารวิชาการนานาชาติ จำนวน 1 ฉบับ ดังนี้**

1. Lomphithak T, Choksi S, Mutirangura A, Tohtong R, Tencomnao T, Hajime U, Michiaki U, Hironobu S, **Jitkaew S*.** Receptor-interacting protein kinase 1 is a key mediator in TLR3 ligand and Smac mimetic-induced cell death and -inhibited invasion in Cholangiocarcinoma Manuscript was submitted.

**2. การนำผลงานวิจัยไปใช้ประโยชน์**

- **ด้านวิชาการ**

การนำเอาเทคโนโลยีคริสเปอร์แคสไนน์ และการตรวจวิเคราะห์การตายของเซลล์โดยใช้ flow cytometer ไปใช้ในการเรียนการสอนปฏิบัติการให้กับนิสิตบัณฑิตศึกษาหลักสูตรชีวเคมีคลินิกและอณูทางการแพทย์ คณะสหเวชศาสตร์ จุฬาลงกรณ์มหาวิทยาลัย นอกจากนั้นองค์ความรู้ที่ได้จากงานวิจัยนี้ยังนำไปต่อยอดโดยการพัฒนาวิธีการรักษาที่จำเพาะต่อโทลล์ไลค์รีเซฟเตอร์สามให้มีประสิทธิภาพมากขึ้น การศึกษากลไกการกระตุ้นระบบภูมิคุ้มกัน และการยับยั้งมะเร็งในสัตว์ทดลอง โดยผู้วิจัยได้รับทุนพัฒนาศักยภาพในการทำงานของอาจารย์รุ่นใหม่ จาก สกอ และสกว ปีงบประมาณ 2564

**3. การนำเสนอผลงานในรูปแบบบรรยายหรือโปสเตอร์ในที่ประชุมวิชาการระดับนานาชาติ**

1. Duangthim N, Sakunpiyanon N, **Jitkaew S***. Generation of Receptor-Interacting Protein Kinase 3 (RIPK3) knockout cholangiocarcinoma cells by CRISPR/Cas9-mediated genome editing. Oral presentation at The 13th Thammasat-Chulalongorn University Medical Technology Student Research International Conference (Best oral presentation award) on January 4, 2017 at Thammasat University, Pathumthani, Thailand.

2. **Jitkaew S***, Lomphithak T, Tohtong T, Sasano H, Mutirangura A. Combination treatment Smac mimetic and TLR3 ligand-induced apoptosis as a novel therapeutic strategy for cholangiocarcinoma. Poster presentation at 17th TRF-OHEC Annual Congress 2019 on January 9-11, 2019 at The regent Cha-am Beach Resort, Phetchaburi, Thailand.

# ภาคผนวก

# Receptor-interacting protein kinase 1 is a key mediator in TLR3 ligand and Smac mimetic-induced cell death and -inhibited invasion in cholangiocarcinoma

Thanpisit Lomphithak[1], Swati Choksi[2], Apiwat Mutirangura[3], Rutaiwan Tohtong[4], Tewin Tencomnao[7], Hajime Usubuchi[5], Michiaki Unno[6], Hironobu Sasano[5], Siriporn Jitkaew[7]*

[1]Graduate Program in Clinical Biochemistry and Molecular Medicine, Department of Clinical Chemistry, Faculty of Allied Health Sciences, Chulalongkorn University, Bangkok, 10330, Thailand.

[2]Center for Cancer Research, National Cancer Institute, 37 Convent Drive, Bethesda, MD, 20892, USA.

[3]Department of Anatomy, Faculty of Medicine, Center of Excellence in Molecular Genetics of Cancer and Human Diseases, Chulalongkorn University, Bangkok 10330

[4]Department of Biochemistry, Faculty of Science, Mahidol University, Bangkok 10400, Thailand

[5]Department of Pathology, Tohoku University School of Medicine, Sendai, Miyagi, 980-8575, Japan

[6]Department of Surgery, Tohoku University School of Medicine, Sendai, Miyagi, 98-8075, Japan

[7]Age-Related Inflammation and Degeneration Research Unit, Department of Clinical Chemistry, Faculty of Allied Health Sciences, Chulalongkorn University, Bangkok, 10330, Thailand.

Siriporn.ji@chula.ac.th

*Corresponding author: Dr. Siriporn Jitkaew
Email address: Siriporn.ji@chula.ac.th
Tel: (66) 022181081, Fax: (66) 022181082

**Running Title:** RIPK1 modulates TLR3-induced cell death and invasion in CCA

**Conflict of Interest.**

The authors declare no conflict of interest.

**Abstract**

Toll-like receptor 3 (TLR3) ligand which activates TLR3 signaling induces both cancer cell death and activates anti-tumor immunity. However, TLR3 signaling can also harbor pro-tumorigenic consequences. Therefore, we examined the status of TLR3 in cholangiocarcinoma (CCA) cases to understand TLR3 signaling and explore the potential target therapy in CCA. TLR3 status was significantly higher in tumor than adjacent normal tissues. Results of subsequent *in vitro* study demonstrated that TLR3 ligand or Poly(I:C) specifically induced CCA cell death, but only when cIAPs were removed by Smac mimetic. Cell death was also switched from apoptosis to necroptosis when caspases were inhibited in CCA cells-expressing RIPK3. In addition, RIPK1 was required for TLR3 ligand and Smac mimetic-induced apoptosis and necroptosis. Of particular interest, high TLR3 or low RIPK1 status was associated with more invasiveness. The loss of RIPK1 enhanced TLR3 ligand-induced invasion through NF-κB/MAPK signaling in *vitro*. Smac mimetic also inhibited TLR3 ligand-induced invasion in RIPK1-dependent manner. Our findings indicated that RIPK1 played pivotal roles in TLR3 signaling and potential therapy targeting TLR3 in combination with Smac mimetic could provide therapeutic benefits to the patients with CCA.

**Keywords:** Toll-like receptor 3, Smac mimetic, RIPK1, cell death, invasion, cholangiocarcinoma

**Abbreviations:** cIAPs, cellular Inhibitor of apoptosis proteins; RIPK1, Receptor-interacting protein kinase 1; RIPK3, Receptor-interacting protein kinase 3; Smac, Second mitochondria-derived activator of caspases

## 1. Introduction

Cholangiocarcinoma (CCA), a markedly heterogeneous malignancy arising from the bile duct epithelium, occurs with a high incidence in Asian countries, but its overall incidence rate is increasing worldwide [1,2]. CCA has relatively high mortality and recurrence/metastasis rate and subsequently poor prognosis. The great majority of CCA patients are usually diagnosed at an advanced stage in which the available treatments are not effective and therefore the better understanding of its molecular pathogenesis and subsequently the discovery of novel therapeutic targets are required to improve the clinical outcome of these patients [2,3]. Chronic inflammation has been generally considered to play pivotal roles in the pathogenesis and/or development of CCA following primary sclerosing cholangitis, parasitic and viral infection, which also indicated the immune related etiology of CCA , and cancer immunotherapy was therefore proposed as an alternative strategy for the treatment of CCA patients [1,2,4]. In addition, development of a novel therapeutic approach which could eliminate cancer cells and reactivate immune responses also result in improving the treatment efficacy, reduce recurrence and increase long-term survival rates of the patients [5].

Toll-like Receptors (TLRs) have become an interesting target for cancer immunotherapy. Among TLRs, Toll-like receptor 3 (TLR3) is one of the promising targets that represents a potential for anti-tumor therapy. TLR3, an endosomal pattern recognition receptor, mediates both innate and adaptive immune responses by sensing viral double-stranded RNA (dsRNA), but also endogenous ligands found at site of damaged tissues and mRNA components released from dying cells [6,7]. TLR3-mediated immune responses is also characterized by the production of inflammatory cytokines and type I interferons (IFNs) [8]. Upon activation, TLR3 signals through an adapter protein called TIR-domain-containing adapter-inducing interferon-β (TRIF also known TICAM

1) which then recruits receptor interacting protein kinase 1 (RIPK1) and TNF receptor-associated factor (TRAF6), thereby leading to the activation of nuclear factor kappaB (NF-κB), mitogen-activated protein kinase (MAPK), and interferon regulatory factor (IRF3) inflammatory signaling pathways [9]. Therefore, TLR3 ligands have successfully been developed and approved at clinical setting as a synthetic dsRNA such as polyinosinic-polycytidylic acid, Poly(I:C), to mimic the response to RNA viral infection [10,11]. In addition, TLR3 ligands have been studied in clinical trials as adjuvants for cancer immunotherapy to enhance cancer vaccine efficacy [12–15]. In addition to orchestrating inflammatory and immune responses, triggering TLR3 signaling by TLR3 ligands has been reported to directly kill various cancer cells such as breast cancer [16,17], melanoma [18,19], renal cell carcinoma [20], prostate cancer [21,22], nasopharyngeal carcinoma [23,24], multiple myeloma [25], head and neck squamous cell carcinoma (HNSCC) [26–28], hepatocellular carcinoma [29], neuroblastoma [30] and non-small cell lung cancer [31,32]. TLR3-mediated cell death is involved the formation of a signaling complex composed of TRIF, RIPK1, Fas-associated protein with death domain (FADD) and caspase-8, the death signaling complex also called ripoptosome [32,33]. RIPK1 represents a key scaffold molecule linking TLR3/TRIF to FADD/caspase-8 signaling cascade which then triggers caspase-8-dependent extrinsic apoptosis [34]. When caspase activity is inhibited, RIPK1 can form a cytosolic death signaling complex with receptor-interacting protein kinase 3 (RIPK3) and mixed lineage kinase domain-like protein (MLKL) which then induces another mode of programmed cell death called necroptosis [35]. As a consequence, necroptotic cell death has been reported to enhance anti-tumor immunity, as in the basic concept of cancer vaccine immunotherapy and is therefore considered an immunogenic cell death (ICD) [36–39]. However, TLR3-mediated necroptosis has not been well explored in cancer cells [40,41].

Negative regulators of TLR3-mediated apoptosis have been also reported in the literature. Cellular inhibitor of apoptosis proteins (cIAPs) including cIAP1 and cIAP2 represent two key molecules that limit TLR3-mediated apoptosis. Both cIAP1 and cIAP2 harbor an interesting new gene (RING) domain E3 ubiquitin ligase [42], thereby mediating RIPK1 poly-ubiquitination resulting in the negative regulation by preventing RIPK1 to form a cytosolic death complex as reported in TNFR1 signaling complex. Therefore, small molecule antagonists of IAPs also known as Smac mimetics have been developed to overcome apoptosis resistance. In TNFR1 signaling complex, Smac mimetics trigger the auto-ubiquitination and proteasomal degradation of E3 ligases cIAP1 and cIAP2 that promote RIPK1 de-ubiquitination, hence its releasing to a cytosolic death signaling complex [43]. Accordingly, Smac mimetics have been reported to sensitize TLR3 ligand-induced apoptosis in some cancer cells [19,24,31–33,44]. Moreover, recent study has demonstrated that the removal of cellular FLICE-like inhibitory protein (c-FLIP), a strong negative regulator of caspase-8-mediated apoptosis could overcome the resistance to TLR3-mediated apoptosis [31].

RIPK1, a serine/threonine kinase is a multifunctional protein that regulates signaling pathways leading to opposing outcomes including inflammation and cell death both in the form of apoptosis and necroptosis [45]. RIPK1 regulates signaling pathways through either kinase-dependent or kinase-independent manner. In addition to TNF-α signaling, RIPK1 has been reported to be also required for TLR3-mediated NF-κB activation [46] and cell death [32,33,47]. The physiological roles of RIPK1 and its regulation have been most extensively studied in TNFR1 signaling but its roles in TLR3 signaling have remained unknown. In addition, whether RIPK1 and its interplay with TLR3 could play a role in CCA and regulate cancer cell invasion has also remained largely unknown [48,49].

TLR3 has been reported as one of novel therapeutic targets that can eliminate cancer cells and activate anti-tumor immunity but TLR3 signaling also acts as a double-edged sword in cancer [50]. Therefore, in this study, we first examined TLR3 status in CCA cases and evaluated its association with clinicopathological parameters of the individual patients in order to search for a novel therapeutic target and also gain a better understanding of TLR3 signaling for improvement of therapeutic approaches targeting TLR3. Therapeutic targeting TLR3 by combination of TLR3 ligand and an IAP antagonist, Smac mimetic to induce cell death and modulate tumor invasion were also investigated in CCA cell lines. In addition, RIPK1 status in CCA cases and its roles in TLR3-mediated cell death as well as its interplay with TLR3 in the modulation of tumorigenic properties such as invasion were also explored in this study.

## 2. Results

### *2.1 TLR3 is differentially expressed in primary CCA tissues and cell lines.*

Stimulation of TLR3 in cancer cells directly induced apoptosis and TLR3 expression in breast cancer patients has been reported to predict clinical responses to TLR3 ligand stimulation [16]. We therefore immunolocalized TLR3 in 88 CCA patients in this study. TLR3 was previously reported to be localized in both the endosomal compartments and on the cell surface. We demonstrated that TLR3 was predominantly immunolocalized in the cytoplasm of human CCA primary tissues (Fig. 1a, Supplementary Fig. 1). The TLR3 immunoreactivity (combined hilar and intrahepatic CCA) was differentially detected in CCA cases (median of H-score of 78.09), while weakly present in adjacent tissues (median of H-score of 38.18) but significantly higher in tumor tissues than adjacent tissues ($p = 2.248E-7$) (Fig. 1b). TLR3 intensity was differentially distributed from negative to strong intensity, compared with adjacent tissues demonstrating mostly negative and low intensity (Fig. 1c, 1d). We then evaluated the TLR3 expression in a panel of CCA cell

lines and immortalized non-tumor cholangiocytes by Western blot analysis. TLR3 was also differentially expressed in all CCA cell lines but not in non-tumor cholangiocytes (Fig. 1e). Collectively, results of our present study demonstrated that TLR3 was differentially expressed in the great majority of CCA patients and all CCA cell lines examined but was restricted to non-tumor cholangiocytes. Therefore, targeting TLR3 signaling could be a novel potential therapeutic target for CCA patients.

*2.2 TLR3 ligand and Smac mimetic induce caspase-8 activation and apoptosis in CCA cell lines.*

In order to explore the sensitivity of CCA cells to TLR3 ligand, Poly(I:C) treatment, we found that none of CCA cell lines that were differentially expressed TLR3 were sensitive to Poly(I:C)-induced cell death (Supplementary Fig. 2). We therefore tentatively hypothesized that the responsiveness to TLR3 ligand stimulation could be possibly influenced by negative regulators including cellular inhibitor of apoptosis proteins (cIAP1 and cIAP2) [33,51] and cellular FLICE-like inhibitory protein (c-FLIP) [31] (Supplementary Fig. 3A, 3B). Therefore, a Smac mimetic (SM-164), an IAP antagonist was combined with Poly(I:C) to enhance the sensitivity towards TLR3-induced cell death. Two of six CCA cell lines examined in this study including KKU100 and KKU213 were the most sensitive to the combination treatment as evaluated by a cell viability, MTT assay followed by KKU214 and RMCCA-1, while KKU-M055 and HuCCT-1 and a non-tumor cholangiocyte, MMNK1 were less sensitive (Supplementary Fig. 4A). We therefore selected KKU100 and KKU213 as two of representative CCA cell lines for the further study, whereas MMNK1 was included as a non-tumor cholangiocyte control. The combination index (CI index) was calculated to indicate the synergistic effects of the combination treatment [52] and the concentration of both Poly(I:C) and Smac mimetic yielding the highest synergistic effect was selected for further experiments (Supplementary Fig. 4B, 4C, 4D). In order to further investigate

whether Poly(I:C) and Smac mimetic specifically triggered apoptosis, more specific apoptosis assays were used to confirm an induction of apoptosis. As in cell viability assay, Poly(I:C) single treatment did not induce cell death, whereas Smac mimetic marginally induced cell death in both KKU100 and KKU213 as evaluated by Annexin V/PI staining (Fig. 2a). However, when Poly(I:C) was combined with Smac mimetic, the cell death was enormously increased in both KKU100 and KKU213, whereas MMNK1 remained completely resistant to Poly(I:C) and Smac mimetic treatment (Fig. 2a). On the contrary, TNF-α and Smac mimetic, a well-known inducer of apoptosis serving as a positive control also enormously induced cell death in MMNK1. In addition, Smac mimetic induced the degradation of cIAP1 and cIAP2 in all the cell lines examined in this study (Supplementary Fig. 5A-D), while Poly(I:C) only triggered the upregulation of TLR3 in CCA cell lines, but not in MMNK1 (Supplementary Fig. 6A-D). The pan-caspase inhibitor, zVAD-fmk completely protected cell death in KKU100, while partially inhibited cell death in KKU213 (Fig. 2a). Consistent with Annexin V/PI staining, activation of caspase-8 (p43/p41 and p18 fragments) and decreased pro-caspase-3 were both detected by Western blot at 6 h and 12 h after the addition of Poly(I:C) and Smac mimetic in both cell lines, and coincided with the cleavage of PARP-1, all characteristic features of apoptosis (Fig. 2b). Altogether, this set of experiments suggested that Poly(I:C) and Smac mimetic combination treatment triggers caspase-8 activation and apoptosis in CCA cell lines.

*2.3 TLR3 ligand and Smac mimetic trigger necroptosis upon caspase inhibition in CCA cell lines.*

TLR3-mediated cell death has been reported to induce not only apoptosis, but also necroptosis in cell lines with RIPK3 expression [40,41]. Therefore, we hypothesized that the combination treatment under the presence of zVAD-fmk (Poly(I:C)/Smac/zVAD-fmk) could switch cell death

mode to necroptosis in CCA cells-expressing RIPK3, since caspase inhibition has previously been reported to cause a switch from apoptosis to necroptosis [53]. To this end, we investigated key necroptotic proteins expression including RIPK1, RIPK3 and MLKL in a panel of CCA cell lines by Western blot analysis. RIPK1 and MLKL were similarly expressed in all CCA cell lines, whereas RIPK3 was only expressed in selected CCA cells including KKU213, RMCCA-1 and HuCCT-1 (Supplementary Fig. 7). Therefore, the partial protection under the presence of zVAD-fmk in KKU213 which expressed RIPK3 might be due to a switch of cell death mode to necroptosis (Fig. 2a) but further investigations are required for clarification. To generalize our results in other CCA cells-expressing RIPK3, we therefore did a pilot study to screen for the sensitivity to Poly(I:C)/Smac/zVAD-fmk-induced cell death, both RMCCA-1 and HuCCT-1 exhibited sensitivity to Poly(I:C)/Smac/zVAD-fmk treatment, while MMNK1 was completely resistant (data not shown). Since the expression of TLR3 in HuCCT-1 was higher than RMCCA-1 and HuCCT-1 was more sensitive to Poly(I:C)/Smac/zVAD-fmk-induced cell death (Fig. 1e, Supplementary Fig. 6D), we therefore selected this cell line for further experiments. Poly(I:C)/Smac/zVAD-fmk significantly induced cell death after 24 h and 48 h in both KKU213 and HuCCT-1 (Fig. 3a). To prove that Poly(I:C)/Smac/zVAD-fmk triggered necroptosis in RIPK3-expressing CCA cell lines, pharmacological inhibitors and genetic disruption of key necroptotic proteins including RIPK3 and MLKL were evaluated in KKU213 and HuCCT-1. Both GSK'872 and necrosulfonamide (NSA), RIPK3 and MLKL inhibitors, respectively reversed Poly(I:C)/Smac/zVAD-fmk-induced cell death in both KKU213 and HuCCT-1 cells, these effects were similar to TNF-α signaling serving as a positive control (Fig. 3b, 3c). In consistence with pharmacological inhibitors, CRISPR/cas9-mediated deletion of *RIPK3* and short hairpins (shRNAs) silencing of MLKL also significantly rescued Poly(I:C)/Smac/zVAD-fmk-induced cell death (Fig.3d, 3e), but did not affect

cell death in the absence of zVAD-fmk (data not shown). The knockout and knockdown efficiency was confirmed by Western blot analysis (Fig. 3d, 3e). Collectively, these results demonstrated that the combination treatment of TLR3 ligand and Smac mimetic in the presence of zVAD-fmk triggers RIPK3- and MLKL-dependent necroptosis.

*2.4 TLR3 ligand and Smac mimetic induce RIPK1 kinase-dependent both apoptosis and necroptosis in CCA cell lines.*

RIPK1 was previously reported to act as a key mediator of TLR3-induced cell death by linking TLR3/TRIF to FADD/caspase-8 death complex [34]. We therefore hypothesized that RIPK1 could play a central mediator of TLR3 ligand and Smac mimetic-induced both apoptosis (Poly(I:C)/Smac) and necroptosis (Poly(I:C)/Smac/zVAD-fmk) in CCA cell lines. Both a pharmacological inhibitor of RIPK1, necrostatin-1 (Nec-1) and a genetic deletion of *RIPK1* were used to explore the involvement of RIPK1. RIPK1 inhibitor (Nec-1) partially abolished Poly(I:C)/Smac-induced apoptosis in both KKU100 and KKU213 cell lines (Fig. 4a, 4b), but the protective effect was more pronounced in KKU100 and KKU213 when *RIPK1* was deleted by CRISPR/cas9 (Fig. 4a, 4b). In addition, both RIPK1 inhibitor (Nec-1) and genetic deletion of *RIPK1* by CRISPR/cas9 almost completely rescued Poly(I:C)/Smac/zVAD-fmk-induced necroptosis in CCA cell lines expressing-RIPK3 including KKU213 and HuCCT-1 (Fig. 4b, 4c). The knockout efficiency of RIPK1 was confirmed by Western blot analysis (Fig. 4a, 4b, 4c). These results all indicated that TLR3 ligand and Smac mimetic induced both apoptosis and necroptosis in a RIPK1 kinase-dependent fashion in CCA cell lines.

*2.5 The association of TLR3 and RIPK1 expression with survival rate in CCA patients.*

RIPK1 represents a key mediator of TLR3 ligand and Smac mimetic induced both apoptosis and necroptosis in CCA cell lines, therefore investigation of RIPK1 in CCA patients became of great importance as an *in vivo* relevance for a potential therapeutic development. Therefore, in this study, RIPK1 was immunolocalized in 88 CCA patients (Fig. 5a, Supplementary Fig. 8). The status of RIPK1 immunoreactivity in the cytoplasm of epithelial or parenchymal cells was significantly higher in CCA tissues than cholangiocytes adjacent to tumor tissues ($p$ = 2.8312E-18) and cholangiocytes from normal liver tissues (Fig. 5b). The relative immunointensity of RIPK1 was low in CCA tissues but negative in adjacent tumor tissues (Fig. 5c, 5d). Kaplan-Meier survival analysis revealed no significant differences between high and low RIPK1 as well as TLR3 expression both disease-free and overall survival rates (Supplementary Fig. 9). Since RIPK1 and TLR3 might cooperatively influence the survival rate of the patients, we then attempted to combine RIPK1 and TLR3 status and tentatively classified into 4 subgroups. However, there were still no significant differences between low and high TLR3/RIPK1 in each subgroup (Fig. 5e). When compared between high TLR3/high RIPK1 and low TLR3/low RIPK1, there was a trend towards a longer disease-free survival in patients with high TLR3 and high RIPK1 ($p$ = 0.078) (Fig. 5f). Altogether, these results indicated that RIPK1 and TLR3 were expressed in a great majority of CCA patients that raises the possibility towards the development targeting TLR3 signaling in combination with Smac mimetic. In addition, patients with high TLR3 and high RIPK1 displayed a trend for a longer disease-free survival.

*2.6 Smac mimetic reverses TLR3 ligand-induced CCA invasion in RIPK1-dependent, but a kinase-independent manner.*

We further analyzed the association of TLR3 or RIPK1 status with clinicopathological parameters by categorizing TLR3 and RIPK1 into high and low expression. As shown in table 1, high TLR3

or low RIPK1 expression was significantly associated with perineural, vascular and lymph node invasions in CCA patients. These results brought us to further explore TLR3 signaling in invasion and the contribution of RIPK1 to this process. *In vitro* matrigel transwell invasion assay was set up in KKU213 with more invasive phenotype. KKU213 was treated with TLR3 ligand, Poly(I:C) and then let the cells growth and invaded for 12 h in transwell insert. As hypothesized, Poly(I:C)-treated KKU213 significantly exhibited higher number of invaded cells than transfection reagent (Turbofect) control groups (Fig. 6a). Poly(I:C)-induced invasion was significantly reduced by NF-κB inhibitor (Bay11-7082), pERK inhibitor (U0126) and pJNK inhibitor (SP600125), but not p38 inhibitor (SB203580) suggesting the involvement of NF-κB and MAPK signaling in Poly(I:C)-induced invasion (Fig. 6a). Since low RIPK1 expression was associated with more invasiveness in CCA patients, we therefore hypothesized that low RIPK1 expression might enhance Poly(I:C)-induced invasion. Consequently, KKU213 RIPK1 knockout cells that were generated previously were used to prove our hypothesis. Of great interest, loss of RIPK1 significantly enhanced Poly(I:C)-induced invasion in NF-κB- and MAPK (pERK, pJNK and p38)- dependent manner (Fig. 6b). Interestingly, when Poly(I:C) was combined with Smac mimetic, the number of invaded cells was significantly lower when compared to Poly(I:C) treatment alone, whereas Smac mimetic did not affect the invaded cells (Fig 6c). All treatment conditions did not influence the cell proliferation or cell viability (Supplementary Fig. 10). The number of invaded cells was significantly higher in KKU213 RIPK1 knockout cells upon the combination treatment of Poly(I:C) and Smac mimetic (Fig 6d, 6e). Similar findings were observed in another CCA cell line, HuCCT-1 (Supplementary Fig. 11). In addition, RIPK1 inhibitor, necrostatin-1 (Nec-1) harbored no effects on Poly(I:C) alone- or Poly(I:C) and Smac mimetic-induced invasion (Fig 6F), suggesting a RIPK1 kinase-independent. Taken together, our results suggested that Smac mimetic

reverses TLR3 ligand-induced CCA invasion in RIPK1-dependent, but a kinase-independent manner.

## 3. Discussions

Targeting TLR3 by TLR3 ligand, Poly(I:C) has become a novel therapeutic strategy in cancer immunotherapy but TLR3 activation in cancer cells could also trigger pro-tumorigenic effects. In this study, we demonstrated the differential and high expression of TLR3 in a great majority of CCA patients and human CCA cell lines. High TLR3 status in tumor tissues was significantly associated with more invasiveness in CCA patients which was also confirmed by subsequent *in vitro* studies that the stimulation of TLR3 by TLR3 ligand, Poly(I:C) promoted CCA cell invasion. Consequently, the potential therapy targeting TLR3 signaling by the combined treatment of TLR3 ligand and an IAPs antagonist, Smac mimetic synergistically induced RIPK1 kinase-dependent apoptosis and necroptosis. As an essential mediator of TLR3-induced cell death, RIPK1 was expressed higher in CCA than the adjacent cholangiocytes in a great majority of CCA patients and low expression of RIPK1 was associated with more invasiveness of carcinoma cells. Of particular interest, Smac mimetic also reversed TLR3 ligand-induced CCA cell invasion in RIPK1-dependent and a kinase-independent manner. *In vivo* data revealed that there was a positive trend between high TLR3 and high RIPK1 with longer disease-free survival ($p = 0.078$). Collectively, this is the very first study to demonstrate that RIPK1 represents a key mediator in TLR3 signaling and therapeutic targeting TLR3 in combination with Smac mimetic could bring a new therapeutic concept with more effective for CCA patients.

We first examined the expression of TLR3 in CCA patients. Consistent with results of the studies in other human malignancies [20,31], results of our present study revealed that a large proportion of CCA patients were differentially expressed TLR3. TLR3 was also differentially expressed in

297 CCA cell lines, but not detected in non-tumor cholangiocytes. Stimulation with TLR3 ligand,
298 Poly(I:C) enhanced TLR3 expression in CCA cell lines, but not in non-tumor cholangiocytes,
299 suggesting that non-tumor cholangiocytes might not be responsive to TLR3 ligand stimulation as
300 TLR3 expression has previously been reported to be induced by TLR3 ligand [18,54], probably
301 through type I IFNs [55]. Therefore, the combination of TLR3 ligand with type I IFNs has been
302 reported to enhance TLR3-induced cell death [17,53]. In addition, TLR3 expression and activation
303 were specific to tumor cells, which could also provide potential rationales for targeting TLR3 with
304 more safe therapy. There have been few data regarding the pro-tumoral roles of TLR3 [56] but
305 the status of TLR3 in carcinoma cells have been reported to predict favorable prognosis in some
306 cancer patients [57,58]. In addition, *in vivo* anti-tumor effects of TLR3 ligand are possibly mainly
307 due to an induction of cell death upon direct stimulation of TLR3 by TLR3 ligand [22] and also
308 the recruitment of tumor-specific CD8+ T lymphocytes [59]. TLR3 ligand stimulation has been
309 reported to induce cell death on itself or combination with sensitizers in several cancers, but lack
310 of evidence in cholangiocarcinoma [16–27,29,31,32,57,60]. Our results did demonstrate for the
311 first time that TLR3 ligand itself did not induce CCA cell death but only in the presence of Smac
312 mimetic, an IAPs antagonist [61], the combination treatment significantly triggered apoptosis with
313 high synergism. Surprisingly, this effect was by no means correlated with TLR3 levels in CCA
314 cells, although TLR3 expression is proposed as a biomarker for the therapeutic efficacy of dsRNA
315 in breast cancer patients [16]. However, it is entirely true that factors that might influence TLR3
316 responsiveness are not known at this juncture. Notably, CCA cell lines that expressed key
317 necroptotic proteins especially RIPK3 exhibited a switch to necroptosis. Necroptosis has been
318 reported to enhance anti-tumor immunity and RIPK3 expression status is proposed to influence
319 the clinical outcome of TLR3-based cancer immunotherapy [40]. The loss of key necroptotic

proteins in cancers has become a major hindrance for necroptosis-based therapy [62,63] but results of our present studies in CCA patients demonstrated that RIPK3 and MLKL were both expressed in a great majority of CCA patients, allowing for the possible development of necroptosis-based therapeutic approaches. Collectively, these results provide a potential for development of a novel therapeutic approach targeting TLR3 in combination with Smac mimetic that can modulate both apoptosis and necroptosis in RIPK1-dependent manner.

RIPK1 is well known to mediate both inflammation and cell death signaling [45], and has emerged as a critical regulator of cell fate determination in response to cellular stress [64]. Our results revealed that RIPK1 was required for TLR3 ligand and Smac mimetic-induced both apoptosis and necroptosis in a kinase-dependent manner, and probably as a scaffold kinase-independent in apoptosis since RIPK1 inhibitor (Nec-1) only partially inhibited apoptosis, but deletion of *RIPK1* almost completely protected apoptosis. The potential roles of RIPK1 in cell death regulation has been extensively reported but its roles in cancers have virtually remained unknown. We further demonstrated that low RIPK1 or high TLR3 in CCA patients was associated with more invasiveness. We therefore hypothesized that TLR3 signaling might promote CCA cell invasion, accordingly *in vitro* invasion assay further supports *in vivo* findings that stimulation of TLR3 by TLR3 ligand promoted CCA cell invasiveness through NF-κB and MAPK signaling. Similar to our findings, stimulation of TLR3 by Poly(I:C) induced migration and invasion in HNSCC and lung cancer [27,65]. Paradoxically, TLR3 ligands have been reported to inhibit the migration in neuroblastoma and hepatocellular carcinoma [29,30]. These results all indicated that TLR3 ligand-induced migration and invasion is cell type-specific and context-dependent. Our results add more roles of RIPK1 in cancer, we show that loss of RIPK1 expression enhanced TLR3 ligand-induced invasion in CCA cells. RIPK1 seems to negatively modulate TLR3 ligand-induced invasion in NF-

κB and MAPK-dependent manner, however the mechanism underlying this effect is currently unclear. In consistent with our study, shRNA silencing of RIPK1 in metastatic HNSCC enhances migration and low RIPK1 expression strongly correlates with metastatic phenotypes in HNSCC patients [49]. In contrast, silencing of RIPK1 expression inhibits invasion in gallbladder carcinoma, therefore RIPK1 might act as a double-edged sword in cancers [48].

TLR3 ligand-induced cancer cell death is a promising anti-cancer therapy, on another side we also demonstrated the pro-tumorigenic consequences of TLR3 ligand, Poly(I:C) that was discussed above. Of great interest, Smac mimetic reversed TLR3-induced CCA cell invasion to basal levels in RIPK1-dependent and a kinase-independent manner, adding more therapeutic benefits of Smac mimetic as a sensitizer of TLR3 ligand treatment. Smac mimetic has been reported to reduce TRAIL-induced invasion and metastasis in CCA cells, partly explained by reducing TRAIL-induced NF-κB activation and thereby matrix metalloproteinase 7 (MMP7) expression [66]. Further studies are needed to investigate how Smac mimetic and RIPK1 collaborate to inhibit invasion in CCA cells. As being targets of Smac mimetic, cIAPs might also contribute to promote invasion in CCA cells, probably through ubiquitination of RIPK1 and in turn leads to NF-κB activation as previously reported for TNF-α signaling [46,67,68]. Our studies in CCA patients demonstrated that high expression of both TLR3 and RIPK1, although not significantly, but there is a trend towards a longer disease-free survival in CCA patients ($p$ = 0.078). Since CCA is associated with chronic inflammation, therefore the activation of TLR3 signaling in response to TLR3 ligands presented in CCA microenvironment might contribute to disease progression, however this pro-tumorigenic signaling might be negatively regulated in the presence of RIPK1. These results provide clinical significance to further support our studies that RIPK1 represents a

key mediator in TLR3 ligand-induced cell death and -inhibited invasion, therefore CCA patients with high TLR3 and high RIPK1 expression could be benefit for this novel treatment concept.

In conclusion, we firstly demonstrated that targeting TLR3 signaling by TLR3 ligand, Poly(I:C) in combination with Smac mimetic induced both apoptosis and necroptosis in CCA cells but restricted to non-tumor cholangiocytes. In addition, Smac mimetic also attenuated TLR3 ligand-induced invasion. Therefore, therapy targeting TLR3 in combination with Smac mimetic could provide a novel therapeutic concept with more effective for CCA patients. More importantly, this is the first study to demonstrate the dual roles of RIPK1 representing a key mediator in this treatment strategy by regulating both cell death and invasion of cancer cells. Finally, we proposed that the patients with high TLR3 and high RIPK1 could benefit greatly for a targeted and personalized therapy.

## Materials and Method

### Cell culture and treatment

Human CCA cell lines (KKU213, KKU100, KKU214, KKU-M055, HuCCT-1) and MMNK1 were obtained from the Japanese Collection of Research Bioresources (JCRB) Cell Bank, Osaka, Japan. RMCCA-1 cells were developed from Thai patients with CCA [69]. All human CCA cell lines and MMNK-1 were cultured in HAM's F-12 medium (HyClone Laboratories, Logan, Utah, USA). All culture media were supplemented with 10% fetal bovine serum (Sigma, St Louis, Missouri, USA) and 1% Penicillin-Streptomycin (HyClone Laboratories, Logan, Utah, USA). All cells were cultured in a humidified incubator at 37 °C with 5% $CO_2$. All cell lines were tested for mycoplasma contamination and were mycoplasma free. For drug treatment, cells were pretreated with Smac mimetic (5 nM for KKU213 or 50 nM for KKU100, HuCCT-1 and MMNK1)

or Smac mimetic and zVAD-fmk (20 μM) for 2 h, after that cells were transfected with 2.5 μg/ml Poly(I:C) by TurboFect transfection reagent (Thermo fisher scientific, Waltham, Massachusetts, USA). Combination index (CI) for Poly(I:C) and Smac mimetic combination treatment was calculated based on Chou-Talalay method using CompuSyn version 1.0 software [52].

**Reagents and antibodies**

Poly(I:C) HMW was purchased from InvivoGen (San Diego, California, USA). Smac mimetic (SM-164) was a gift from S. Wang (University of Michigan, Ann Arbor, Michigan, USA). Pan-caspase inhibitor (z-VAD-FMK), GSK'782, necrosulfonamide (NSA), Bay11-7082, U0126, SP600125 and SB203580 were purchased from Calbiochem (Merck Millipore, Darmstadt, Germany). Necrostatin-1 (Nec-1) were purchased from Sigma (St Louis, Missouri, USA). TNF-α was purchased from R&D systems (Minneapolis, Minnesota, USA). Antibodies for Western blot were purchased from commercial available providers as following: anti-RIPK1 (610459) was from BD Biosciences (San Jose, California, USA); anti-TLR3 (6961), anti-RIPK3 (8457), anti-cIAP1 (7065), anti-cIAP2 (3130), anti-caspase-8 (9746), anti-caspase-3 (9662), anti-PARP-1 (9542) and anti-actin (4970) were from Cell signaling (Danvers, Massachusetts, USA); anti-MLKL (ab184718) were from Abcam (Cambridge, UK).

**Patient samples**

Formalin-fixed and paraffin-embedded tumor blocked were obtained from 88 CCA patients (Intrahepatic CCA = 21 samples and Hilar CCA = 67 samples) whose primary tumor were surgically resected between 2005 and 2015 at Tohoku University Hospital, Sendai, Japan Clinicopathological parameters of individual patient were detailed in Table 1. The study protocol

was approved by IRB of Tohoku University School of Medicine, Sendai, Japan. Informed consent was obtained.

**Immunohistochemical staining and evaluation**

Paraffin-embedded CCA sections were deparaffinized and hydrated in xylene and ethanol respectively, then autoclaved for 5 min in an antigen retrieval solution, sodium citrate buffer (pH 6.0). Tissue sections were incubated overnight at 4°C with primary antibodies, including mouse monoclonal anti-TLR3 (1:500 dilution; ab13915; Abcam, Cambridge, UK) and mouse anti-RIP (1:200 dilution; 610459; BD Biosciences, San Jose, California, USA). Tissue sections were then incubated with biotinylated secondary. After that, peroxidase activity was developed with 3,30-diaminobenzidine tetrahydrochloride and counterstained with hematoxylin. Tissue sections were then sealed with neutral resins.

Stained slides were evaluated by light microscopy by two individuals (HU and TL). All tissue sections were scored in a semi-quantitative manner. Intensity was classified as 0 (no-stain), +1 (weak staining), +2 (moderate staining) or +3 (strong staining). A value H-score was obtained for each slide by using the following formula: H-score = (%Strong x 3) + (%Moderate x 2) + %Weak. TLR3 and RIPK1 expression were classified by H-score, weak (< 100), moderate (100-200) and strong (> 200). Low and high TLR3 or RIPK1 expression were divided based on the median H-score of all specimens.

**CRISPR plasmid, shRNAs and Lentivirus infection**

CRISPR plasmids targeting human RIPK1 (NM_003804) and human RIPK3 (NM_006871) were generated following to Zhang's protocol. The sequence for CRISPR-RIPK1 was 5'-CACCGGA TGCACGTGCTGAAAGCCG-3' and CRISPR-RIPK3 was 5'-CAGTGTTCCGGGCGCAAAT-

3'. The shRNAs against human MLKL (NM_152649.4) corresponding to the 3' untranslated region 2025-2045 (shMLKL1) and 1907-1927 (shMLKL2) were purchased from Sigma (St Louis, Missouri, USA). All plasmid constructs were subsequently confirmed by DNA sequencing. HEK293T cells were used to generate lentiviral particles, by co-transfection of packaging plasmid (pCMV-VSV-G) and envelope plasmid (pCMV-dr8.2-dvpr) and either CRISPR-V2 or CRISPR-RIPK1 or CRISPR-RIPK3 plasmids or shRNA-non-targeting (shNT; pLKO.1puro) and shRNA-MLKL (shMLKL). After 24 h, supernatants containing viral particles were collected and filtered through a 0.45 μM sterile filter membrane (Merck Millipore, Darmstadt, Germany). Eight μg/mL of polybrene (Merck Millipore, Darmstadt, Germany) was added to the lentiviral preparation and then used to infect the cells. After 24 h of infection, the cells were selected with puromycin (Merck Millipore, Darmstadt, Germany) for a further 48 h.

**Western blot analysis**

Western blot analysis was performed according to previously described in [12]. Cells were lysed in RIPA buffer (Merck Millipore, Darmstadt, Germany) containing a proteinase inhibitor cocktail (Roche, Mannheim, Germany). Total proteins were separated by 10% or 12% SDS-PAGE and proteins were transferred onto PVDF membranes. The membranes were incubated with the primary antibodies listed above. The proteins were visualized by enhanced chemiluminescence according to the manufacturer's instructions (Bio-Rad, Hercules, California, USA). All Western blots shown were representative of at least three independent experiments.

**AnnexinV and Propidium Iodide (PI) staining**

Cell death was assessed by AnnexinV and PI dual staining using Flow cytometry. Briefly, cells were collected and resuspended in Annexin V binding buffer containing recombinant Annexin V-

FITC (ImmunoTools, Friesoythe, Germany) and PI (Invitrogen; Thermo Fisher Scientific, Inc., California, USA). The stained cells were analyzed with flow cytometry (Navios, Beckman Coulter, Indianapolis, USA).

**Transwell invasion Assay**

Transwell insert was pre-coated with 50 μg/well of Matrigel (Corning, Tewksbury, Massachusetts, USA). Cells in serum free media were seeded in the upper Transwell chambers (Corning, Tewksbury, Massachusetts, USA). Complete medium was added to the lower chamber. The plates were incubated at 37 °C, 5% $CO_2$. After 12 h, the invaded cells were fixed with 4% formaldehyde and stained with 0.1% crystal violet. Number of invaded cells were counted in 5 random fields.

**Statistical analysis**

All statistical analyses were conducted using the software package SPSS for Windows. The Pearson's $\chi 2$ was used to analyze the association of clinicopathological factors and TLR3 or RIPK1 expression. Disease free and overall survival of patients were estimated by Kaplan-Meier method using log-rank test. Results were expressed as the mean ± standard deviation (S.D.) of at least three independent experiments. Comparisons between two groups were determined by a two-tailed Student's t-tests. All *p*-values less than 0.05 were considered statistically significant.

**Acknowledgements**

This work was supported by grants from the Research Grant for New Scholar by The Thailand Research Fund and Office of the Higher Education Commission (MRG6080130) and Grants for Development of New Faculty Staff, Ratchadaphiseksomphot Endowment Fund (DNS 61-004-37-001-2) to SJ. TL is gratefully acknowledged the Scholarship from the Graduate School,

Chulalongkorn University to commemorate the 72nd anniversary of his Majesty King Bhumibol Aduladej (GCUGE12-2), the Chulalongkorn University 90th Anniversary Fund and Join Funding (Ratchadaphiseksomphot Endowment Fund) (GCUGR1125613083M). We thank Dr. Zheng-Gang Liu (NIH, Maryland, USA) for providing useful antibodies and reagents, lentiviral expression system and CRISPR backbone construct. We thank Assist. Prof. Dr. Panthip Rattanasinganchan (Huachiew Chalermprakiet University) and Asst. Prof. Dr. Chanchai Boonla (Chulalongkorn University) for kindly provided; HuCCT-1; and KKU214, respectively.

**Conflict of Interest.**

The authors declare no conflict of interest.

**Author contributions**

TL performed the experiments, analyzed the data, organized the figures and drafted the manuscript under the supervision of SJ.

SC provided reagents and antibodies and revised the manuscript.

RT provided CCA cell lines and was involved in critical review of the manuscript.

AM, TT provided reagents and antibodies and were involved in critical review of the manuscript.

HU performed and analyzed immunohistochemistry data.

HS provided CCA clinical samples and revised the manuscript.

SJ conceived and designed the experiments, analyzed and interpreted the data and wrote the manuscript.

All authors read and approved the final version of the manuscript.

**Figure legend**

**Fig. 1** TLR3 is differentially expressed in primary CCA tissues and cell lines. (**A**) The representative cytoplasmic TLR3 immunostaining in tumor area and adjacent normal tissues. Black arrowheads indicate bile ducts. (**B**) The median of H-score of staining in CCA primary tissues (tumor tissues and adjacent). Distribution of TLR3 expression according to H-score of (**C**) tumor area and (**D**) adjacent. (**E**) Protein expression of TLR3 was analyzed in 6 different human CCA cell lines and an immortalized human cholangiocyte cell line, MMNK1 using Western blot analysis and β-actin was served as loading control.

**Fig. 2** TLR3 ligand and Smac mimetic induce caspase-8-dependent apoptosis in CCA cell lines. (**A**) MMNK1, KKU100, and KKU213 cells were pretreated with Smac mimetic (50 nM MMNK1 and KKU100, and 5 nM KKU213) (Smac) or Smac mimetic and 20 μM zVAD-fmk (SZ) for 2 h. After that the cells were transfected with 2.5 μg/ml Poly(I:C) (PS, PSZ) for 24 h. TNF-α at 10 ng/ml and Smac mimetic or zVAD-fmk at the same concentration as with Poly(I:C) (TS, TSZ) were used as a positive control. Cell death was determined by Annexin V and propidium iodide staining followed by flow cytometry. Data from three independent experiments was presented as mean $\pm$ S.D.; * $p < 0.05$, ** $p < 0.01$, *** $p < 0.001$ (**B**) KKU100 and KKU213 cells were treated as in (A) for 6 h and 12 h. Cell lysates were collected, after that activation of caspase-8 and caspase-3 and cleavage of PARP-1 were analyzed by Western blot analysis. β-actin was served as loading control. Data shown was a representative of two independent experiments.

**Fig. 3** TLR3 ligand and Smac mimetic trigger necroptosis upon caspase inhibition in CCA cell lines. (**A**) RIPK3-expressing cells, KKU213 and HuCCT-1 were pretreated with 20 μM zVAD-fmk and Smac mimetic (5 nM KKU213 and 50 nM HuCCT-1) for 2 h. The cells were transfected

with 2.5 μg/ml Poly(I:C) for 24 h and 48 h. TNF-α/zVAD-fmk/Smac mimetic (TSZ) were represented as a positive control. KKU213 (left) and HuCCT-1 (right) cells were pretreated with 10 μM RIPK3 inhibitor (GSK'872) (**B**) or 1 μM MLKL inhibitor (NSA) (**C**) for 2 h. At the same time, the cells were pretreated with zVAD-fmk and Smac mimetic (SZ). After that the cells were treated as in (A). (**D**) KKU213 and HuCCT-1 cells-expressing CRISPR control (CRISPR-V2) or CRISPR-RIPK3 (RIPK3) were treated as in (A) for 24 h. The representative knockout efficiency was shown on right. (**E**) KKU213 and HuCCT-1 cells-expressing shRNA control (shNT) or shRNAs targeting two different sequences of MLKL (shMLKL1, shMLKL2) were treated as in (A). The representative knockdown efficiency was shown on right. Cell death was determined by Annexin V and PI staining and flow cytometry. Data from three independent experiments was presented as mean ± S.D.; * $p < 0.05$, ** $p < 0.01$, *** $p < 0.001$.

**Fig. 4** TLR3 ligand and Smac mimetic induce RIPK1-dependent apoptosis and necroptosis in CCA cell lines. (**A**) KKU100 cells were pretreated with 60 μM RIPK1 inhibitor (Nec-1, necrostatin-1) and 50 nM Smac mimetic for 2 h followed by transfection with 2.5 μg/ml Poly(I:C) (PS) or treatment with 10 ng/ml TNF-α (TS) (positive control) for 24 h. (**B**) KKU100 cells-expressing CRISPR control (CRISPR-V2) or CRISPR-RIPK1 (RIPK1) were pretreated with 50 nM Smac mimetic for 2 h followed by treatment as in (A) for 24 h. (**C**) KKU213 cells was treated as in (A) except for Smac mimetic was used at 5 nM and zVAD-fmk was also included. (**D**) KKU213 cells-expressing CRISPR control (CRISPR-V2) or CRISPR-RIPK1 (RIPK1) were treated as in (B). (**E**) HuCCT-1 cells were pretreated with 50 nM Smac mimetic and zVAD-fmk for 2 h, followed by transfection with 2.5 μg/ml Poly(I:C) (PSZ) or treated with 10 ng/ml TNF-α (TSZ) (positive control) for 24 h. (**F**) HuCCT-1 cells-expressing CRISPR control (CRISPR-V2) or CRISPR-RIPK1 (RIPK1) were treated as in (E) for 24 h. The representative knockout efficiency in (B)

KKU100, (E) KKU213, and (F) HuCCT-1 cells were shown on right. Cell death was determined by Annexin V and PI staining and flow cytometry. Data from three independent experiments was presented as mean ± S.D.; * $p < 0.05$, ** $p < 0.01$, *** $p < 0.001$.

**Fig. 5** The association of TLR3 and RIPK1 expression with survival rate in CCA patients. (**A**) The representative cytoplasmic RIPK1 immunostaining in tumor area and adjacent normal tissues. Black arrowheads indicate bile ducts. (**B**) The median of H-score of RIPK1 staining in tumor area, adjacent normal tissues and cholangiocytes, liver cells in normal liver tissues. Distribution of RIPK1 expression according to H-score of (**C**) tumor area and (**D**) adjacent. RIPK1 and TLR3 expression were classified into four groups according to low and high expression. Kaplan-Meier disease free survival curves stratified by (**E**) four groups of TLR3 and RIPK1 expression (Low Low, High High, Low High, High Low) and (**F**) two groups of TLR3 and RIPK1 expression (High High, Low Low).

**Fig. 6** Smac mimetic reverses TLR3 ligand-induced invasion in RIPK1-dependent manner. (**A**) KKU213 cells were pretreated with 10 μM Bay11-7082, 10 μM U0126, 20 μM SP600125 or 10 μM SB203580 for 30 min followed by transfection with TurboFect or 2.5 μg/ml Poly(I:C) for 12 h and then subjected to invasion assays. (**B**) Quantification of number of CRISPR-V2 and CRISPR-RIPK1 KKU213 invaded cells. (**C**) Representative images of CRISPR-V2 and CRISPR-RIPK1 invaded cells stained with crystal violet. (**D**) KKU213 cells were pretreated with 5 nM Smac mimetic followed by transfection with 2.5 μg/ml Poly(I:C) for 12 h. (**E**) Quantification of number of CRISPR-V2 and CRISPR-RIPK1 KKU213 invaded cells treated with 5 nM Smac mimetic, 2.5 μg/ml Poly(I:C) alone or the combination treatment for 12 h. (**D**) KKU213 cells were pretreated with RIPK1 inhibitor (Nec-1) with or without 5 nM Smac mimetic followed by transfection with 2.5 μg/ml Poly(I:C) for 12 h. Number of invaded cells were counted. Data from

three independent experiments was presented as mean ± S.D.; * $p < 0.05$, ** $p < 0.01$, *** $p < 0.001$, n.s. = not significant

**Fig. 7** RIPK1 modulates TLR3-induced cell death and invasion in CCA. (**A**) In CCA cells with RIPK1 and TLR3 expression, Smac mimetic and TLR3 ligand, Poly(I:C) induces apoptosis and necroptosis and inhibits invasion in RIPK1-dependent manner. (**B**) In CCA cells with low RIPK1 expression, Smac mimetic and TLR3 ligand-induced apoptosis and necroptosis are inhibited, while invasion is enhanced.

**Table 1** Associations of RIPK1 and TLR3 expression with clinicopathological parameters of CCA patients.

## References

[1] J.M. Banales, V. Cardinale, G. Carpino, M. Marzioni, J.B. Andersen, P. Invernizzi, G.E. Lind, T. Folseraas, S.J. Forbes, L. Fouassier, A. Geier, D.F. Calvisi, J.C. Mertens, M. Trauner, A. Benedetti, L. Maroni, J. Vaquero, R.I.R. Macias, C. Raggi, M.J. Perugorria, E. Gaudio, K.M. Boberg, J.J.G. Marin, D. Alvaro, Cholangiocarcinoma: current knowledge and future perspectives consensus statement from the European Network for the Study of Cholangiocarcinoma (ENS-CCA), Nat. Rev. Gastroenterol. Hepatol. 13 (2016) 261–280. doi:10.1038/nrgastro.2016.51.

[2] S. Rizvi, S.A. Khan, C.L. Hallemeier, R.K. Kelley, G.J. Gores, Cholangiocarcinoma — evolving concepts and therapeutic strategies, Nat. Rev. Clin. Oncol. 15 (2017) 95–111. doi:10.1038/nrclinonc.2017.157.

[3] J.J.G. Marin, E. Lozano, O. Briz, R. Al-Abdulla, M.A. Serrano, R.I.R. Macias, Molecular Bases of Chemoresistance in Cholangiocarcinoma, Curr. Drug Targets. 18 (2017) 889–

900. doi:10.2174/138945011666615022312150 8.

[4] G. Landskron, M. De la Fuente, P. Thuwajit, C. Thuwajit, M.A. Hermoso, Chronic Inflammation and Cytokines in the Tumor Microenvironment, J. Immunol. Res. 2014 (2014) 1–19. doi:10.1155/2014/149185.

[5] P. Gotwals, S. Cameron, D. Cipolletta, V. Cremasco, A. Crystal, B. Hewes, B. Mueller, S. Quaratino, C. Sabatos-Peyton, L. Petruzzelli, J.A. Engelman, G. Dranoff, Prospects for combining targeted and conventional cancer therapy with immunotherapy, Nat. Rev. Cancer. 17 (2017) 286–301. doi:10.1038/nrc.2017.17.

[6] A. Marshak-Rothstein, Toll-like receptors in systemic autoimmune disease, Nat. Rev. Immunol. 6 (2006) 823–835. doi:10.1038/nri1957.

[7] K. Karikó, H. Ni, J. Capodici, M. Lamphier, D. Weissman, mRNA is an endogenous ligand for Toll-like receptor 3., J. Biol. Chem. 279 (2004) 12542–50. doi:10.1074/jbc.M310175200.

[8] F. Bianchi, S. Pretto, E. Tagliabue, A. Balsari, L. Sfondrini, Exploiting poly(I:C) to induce cancer cell apoptosis, Cancer Biol. Ther. 18 (2017) 747–756. doi:10.1080/15384047.2017.1373220.

[9] T. Kawasaki, T. Kawai, Toll-Like Receptor Signaling Pathways, Front. Immunol. 5 (2014) 461. doi:10.3389/fimmu.2014.00461.

[10] A.S. Levine, H.B. Levy, Phase I-II trials of poly IC stabilized with poly-L-lysine., Cancer Treat. Rep. 62 (1978) 1907–12. http://www.ncbi.nlm.nih.gov/pubmed/728910 (accessed February 18, 2019).

606 [11] L. Galluzzi, E. Vacchelli, A. Eggermont, W.H. Fridman, J. Galon, C. Sautès-Fridman, E.
607 Tartour, L. Zitvogel, G. Kroemer, Trial Watch, Oncoimmunology. 1 (2012) 306–315.
608 doi:10.4161/onci.19549.

609 [12] Q. Xu, S. Jitkaew, S. Choksi, C. Kadigamuwa, J. Qu, M. Choe, J. Jang, C. Liu, Z. Liu,
610 The cytoplasmic nuclear receptor RARγ controls RIP1 initiated cell death when cIAP
611 activity is inhibited, Nat. Commun. 8 (2017) 425. doi:10.1038/s41467-017-00496-6.

612 [13] M.E. Rodríguez-Ruiz, J.L. Perez-Gracia, I. Rodríguez, C. Alfaro, C. Oñate, G. Pérez, I.
613 Gil-Bazo, A. Benito, S. Inogés, A. López-Diaz de Cerio, M. Ponz-Sarvise, L. Resano, P.
614 Berraondo, B. Barbés, S. Martin-Algarra, A. Gúrpide, M.F. Sanmamed, C. de Andrea,
615 A.M. Salazar, I. Melero, Combined immunotherapy encompassing intratumoral poly-
616 ICLC, dendritic-cell vaccination and radiotherapy in advanced cancer patients, Ann.
617 Oncol. 29 (2018) 1312–1319. doi:10.1093/annonc/mdy089.

618 [14] A.M. Salazar, R.B. Erlich, A. Mark, N. Bhardwaj, R.B. Herberman, Therapeutic In Situ
619 Autovaccination against Solid Cancers with Intratumoral Poly-ICLC: Case Report,
620 Hypothesis, and Clinical Trial, Cancer Immunol. Res. 2 (2014) 720–724.
621 doi:10.1158/2326-6066.CIR-14-0024.

622 [15] H. Okada, P. Kalinski, R. Ueda, A. Hoji, G. Kohanbash, T.E. Donegan, A.H. Mintz, J.A.
623 Engh, D.L. Bartlett, C.K. Brown, H. Zeh, M.P. Holtzman, T.A. Reinhart, T.L. Whiteside,
624 L.H. Butterfield, R.L. Hamilton, D.M. Potter, I.F. Pollack, A.M. Salazar, F.S. Lieberman,
625 Induction of CD8 $^{+}$ T-Cell Responses Against Novel Glioma–Associated Antigen Peptides
626 and Clinical Activity by Vaccinations With α-Type 1 Polarized Dendritic Cells and
627 Polyinosinic-Polycytidylic Acid Stabilized by Lysine and Carboxymethylcellulose in

628 Patients With Recurrent Malignant Glioma, J. Clin. Oncol. 29 (2011) 330–336.
629 doi:10.1200/JCO.2010.30.7744.

630 [16] B. Salaun, L. Zitvogel, C. Asselin-Paturel, Y. Morel, K. Chemin, C. Dubois, C.
631 Massacrier, R. Conforti, M.P. Chenard, J.-C. Sabourin, A. Goubar, S. Lebecque, M.
632 Pierres, D. Rimoldi, P. Romero, F. Andre, TLR3 as a Biomarker for the Therapeutic
633 Efficacy of Double-stranded RNA in Breast Cancer, Cancer Res. 71 (2011) 1607–1614.
634 doi:10.1158/0008-5472.CAN-10-3490.

635 [17] B. Salaun, I. Coste, M.-C. Rissoan, S.J. Lebecque, T. Renno, TLR3 can directly trigger
636 apoptosis in human cancer cells., J. Immunol. 176 (2006) 4894–901.
637 doi:10.4049/JIMMUNOL.176.8.4894.

638 [18] B. Salaun, S. Lebecque, S. Matikainen, D. Rimoldi, P. Romero, Toll-like Receptor 3
639 Expressed by Melanoma Cells as a Target for Therapy?, Clin. Cancer Res. 13 (2007)
640 4565–4574. doi:10.1158/1078-0432.CCR-07-0274.

641 [19] A. Weber, Z. Kirejczyk, R. Besch, S. Potthoff, M. Leverkus, G. Häcker, Proapoptotic
642 signalling through Toll-like receptor-3 involves TRIF-dependent activation of caspase-8
643 and is under the control of inhibitor of apoptosis proteins in melanoma cells, Cell Death
644 Differ. 17 (2010) 942–951. doi:10.1038/cdd.2009.190.

645 [20] T. Morikawa, A. Sugiyama, H. Kume, S. Ota, T. Kashima, K. Tomita, T. Kitamura, T.
646 Kodama, M. Fukayama, H. Aburatani, Identification of Toll-Like Receptor 3 as a
647 Potential Therapeutic Target in Clear Cell Renal Cell Carcinoma, Clin. Cancer Res. 13
648 (2007) 5703–5709. doi:10.1158/1078-0432.CCR-07-0603.

649 [21] A. Paone, D. Starace, R. Galli, F. Padula, P. De Cesaris, A. Filippini, E. Ziparo, A.

650 Riccioli, Toll-like receptor 3 triggers apoptosis of human prostate cancer cells through a
651 PKC-a-dependent mechanism, Carcinogenesis. 29 (2008) 1334–1342.
652 doi:10.1093/carcin/bgn149.

653 [22] G. Gambara, M. Desideri, A. Stoppacciaro, F. Padula, P. De Cesaris, D. Starace, A.
654 Tubaro, D. del Bufalo, A. Filippini, E. Ziparo, A. Riccioli, TLR3 engagement induces
655 IRF-3-dependent apoptosis in androgen-sensitive prostate cancer cells and inhibits tumour
656 growth *in vivo*, J. Cell. Mol. Med. 19 (2015) 327–339. doi:10.1111/jcmm.12379.

657 [23] B. Vérillaud, M. Gressette, Y. Morel, C. Paturel, P. Herman, K. Lo, S. Tsao, M. Wassef,
658 A.-S. Jimenez-Pailhes, P. Busson, Toll-like receptor 3 in Epstein-Barr virus-associated
659 nasopharyngeal carcinomas: consistent expression and cytotoxic effects of its synthetic
660 ligand poly(A:U) combined to a Smac-mimetic, Infect. Agent. Cancer. 7 (2012) 36.
661 doi:10.1186/1750-9378-7-36.

662 [24] L. Friboulet, C. Pioche-Durieu, S. Rodriguez, A. Valent, S. Souquère, H. Ripoche, A.
663 Khabir, S. Wah Tsao, J. Bosq, K. Wai Lo, P. Busson, H. Kong Hong Kong, Recurrent
664 Overexpression of c-IAP2 in EBV-Associated Nasopharyngeal Carcinomas: Critical Role
665 in Resistance to Toll-like Receptor 3-Mediated Apoptosis 1,2, Neoplasia. 10 (2008) 1183.
666 doi:10.1593/neo.08590.

667 [25] D. Chiron, C. Pellat-Deceunynck, M. Amiot, R. Bataille, G. Jego, TLR3 Ligand Induces
668 NF- B Activation and Various Fates of Multiple Myeloma Cells Depending on
669 IFN- Production, J. Immunol. 182 (2009) 4471–4478. doi:10.4049/jimmunol.0803113.

670 [26] N. Nomi, S. Kodama, M. Suzuki, Toll-like receptor 3 signaling induces apoptosis in
671 human head and neck cancer via survivin associated pathway., Oncol. Rep. 24 (2010)

672 225–31. http://www.ncbi.nlm.nih.gov/pubmed/20514466 (accessed February 18, 2019).

673 [27] C. Rydberg, A. Månsson, R. Uddman, K. Riesbeck, L.-O. Cardell, Toll-like receptor
674 agonists induce inflammation and cell death in a model of head and neck squamous cell
675 carcinomas., Immunology. 128 (2009) e600-11. doi:10.1111/j.1365-2567.2008.03041.x.

676 [28] N. Umemura, J. Zhu, Y.K. Mburu, A. Forero, P.N. Hsieh, R. Muthuswamy, P. Kalinski,
677 R.L. Ferris, S.N. Sarkar, Defective NF- B Signaling in Metastatic Head and Neck Cancer
678 Cells Leads to Enhanced Apoptosis by Double-Stranded RNA, Cancer Res. 72 (2012) 45–
679 55. doi:10.1158/0008-5472.CAN-11-1484.

680 [29] L. Chen, L. Chen, Y. Zhu, Y. Zhang, S. He, J. Qin, X. Tang, J. Zhou, Y. Wei, Double-
681 stranded RNA-induced TLR3 activation inhibits angiogenesis and triggers apoptosis of
682 human hepatocellular carcinoma cells, Oncol. Rep. 27 (2011) 396–402.
683 doi:10.3892/or.2011.1538.

684 [30] W.-M. Hsu, C.-C. Huang, H.-Y. Lee, P.-Y. Wu, M.-T. Wu, H.-C. Chuang, L.-L. Lin, J.-H.
685 Chuang, MDA5 complements TLR3 in suppression of neuroblastoma., Oncotarget. 6
686 (2015) 24935–46. doi:10.18632/oncotarget.4511.

687 [31] L. Alkurdi, F. Virard, B. Vanbervliet, K. Weber, F. Toscano, M. Bonnin, N. Le Stang, S.
688 Lantuejoul, O. Micheau, T. Renno, S. Lebecque, Y. Estornes, Release of c-FLIP brake
689 selectively sensitizes human cancer cells to TLR3-mediated apoptosis., Cell Death Dis. 9
690 (2018) 874. doi:10.1038/s41419-018-0850-0.

691 [32] Y. Estornes, F. Toscano, F. Virard, G. Jacquemin, A. Pierrot, B. Vanbervliet, M. Bonnin,
692 N. Lalaoui, P. Mercier-Gouy, Y. Pachéco, B. Salaun, T. Renno, O. Micheau, S. Lebecque,
693 dsRNA induces apoptosis through an atypical death complex associating TLR3 to

caspase-8, Cell Death Differ. 19 (2012) 1482–1494. doi:10.1038/cdd.2012.22.

[33] M. Feoktistova, P. Geserick, B. Kellert, D.P. Dimitrova, C. Langlais, M. Hupe, K. Cain, M. MacFarlane, G. Häcker, M. Leverkus, cIAPs Block Ripoptosome Formation, a RIP1/Caspase-8 Containing Intracellular Cell Death Complex Differentially Regulated by cFLIP Isoforms, Mol. Cell. 43 (2011) 449–463. doi:10.1016/j.molcel.2011.06.011.

[34] N.S. Wilson, V. Dixit, A. Ashkenazi, Death receptor signal transducers: nodes of coordination in immune signaling networks, Nat. Immunol. 10 (2009) 348–355. doi:10.1038/ni.1714.

[35] T. Vanden Berghe, A. Linkermann, S. Jouan-Lanhouet, H. Walczak, P. Vandenabeele, Regulated necrosis: the expanding network of non-apoptotic cell death pathways, Nat. Rev. Mol. Cell Biol. 15 (2014) 135–147. doi:10.1038/nrm3737.

[36] N. Yatim, H. Jusforgues-Saklani, S. Orozco, O. Schulz, R. Barreira da Silva, C. Reis e Sousa, D.R. Green, A. Oberst, M.L. Albert, RIPK1 and NF- B signaling in dying cells determines cross-priming of CD8+ T cells, Science (80-. ). 350 (2015) 328–334. doi:10.1126/science.aad0395.

[37] T.L. Aaes, A. Kaczmarek, T. Delvaeye, B. De Craene, S. De Koker, L. Heyndrickx, I. Delrue, J. Taminau, B. Wiernicki, P. De Groote, A.D. Garg, L. Leybaert, J. Grooten, M.J.M. Bertrand, P. Agostinis, G. Berx, W. Declercq, P. Vandenabeele, D.V. Krysko, Vaccination with Necroptotic Cancer Cells Induces Efficient Anti-tumor Immunity, Cell Rep. 15 (2016) 274–287. doi:10.1016/j.celrep.2016.03.037.

[38] O. Krysko, T.L. Aaes, V.E. Kagan, K. D'Herde, C. Bachert, L. Leybaert, P. Vandenabeele, D. V. Krysko, Necroptotic cell death in anti-cancer therapy, Immunol.

716 Rev. 280 (2017) 207–219. doi:10.1111/imr.12583.

717 [39] N. Yatim, S. Cullen, M.L. Albert, Dying cells actively regulate adaptive immune
718 responses, Nat. Rev. Immunol. 17 (2017) 262–275. doi:10.1038/nri.2017.9.

719 [40] S. V. Schmidt, S. Seibert, B. Walch-Rückheim, B. Vicinus, E.-M. Kamionka, J. Pahne-
720 Zeppenfeld, E.-F. Solomayer, Y.-J. Kim, R.M. Bohle, S. Smola, RIPK3 expression in
721 cervical cancer cells is required for PolyIC-induced necroptosis, IL-1α
722 release, and efficient paracrine dendritic cell activation, Oncotarget. 6 (2015) 8635–47.
723 doi:10.18632/oncotarget.3249.

724 [41] R. Takemura, H. Takaki, S. Okada, H. Shime, T. Akazawa, H. Oshiumi, M. Matsumoto,
725 T. Teshima, T. Seya, PolyI:C-Induced, TLR3/RIP3-Dependent Necroptosis Backs Up
726 Immune Effector-Mediated Tumor Elimination In Vivo, Cancer Immunol. Res. 3 (2015)
727 902–914. doi:10.1158/2326-6066.CIR-14-0219.

728 [42] S. Fulda, D. Vucic, Targeting IAP proteins for therapeutic intervention in cancer, Nat.
729 Rev. Drug Discov. 11 (2012) 109–124. doi:10.1038/nrd3627.

730 [43] M. Gyrd-Hansen, P. Meier, IAPs: from caspase inhibitors to modulators of NF-κB,
731 inflammation and cancer, Nat. Rev. Cancer. 10 (2010) 561–574. doi:10.1038/nrc2889.

732 [44] S.T. Beug, V.A. Tang, E.C. LaCasse, H.H. Cheung, C.E. Beauregard, J. Brun, J.P.
733 Nuyens, N. Earl, M. St-Jean, J. Holbrook, H. Dastidar, D.J. Mahoney, C. Ilkow, F. Le
734 Boeuf, J.C. Bell, R.G. Korneluk, Smac mimetics and innate immune stimuli synergize to
735 promote tumor death, Nat. Biotechnol. 32 (2014) 182–190. doi:10.1038/nbt.2806.

736 [45] K. Newton, RIPK1 and RIPK3: critical regulators of inflammation and cell death, Trends

Cell Biol. 25 (2015) 347–353. doi:10.1016/j.tcb.2015.01.001.

[46] E. Meylan, K. Burns, K. Hofmann, V. Blancheteau, F. Martinon, M. Kelliher, J. Tschopp, RIP1 is an essential mediator of Toll-like receptor 3–induced NF-κB activation, Nat. Immunol. 5 (2004) 503–507. doi:10.1038/ni1061.

[47] D. Ofengeim, J. Yuan, Regulation of RIP1 kinase signalling at the crossroads of inflammation and cell death, Nat. Rev. Mol. Cell Biol. 14 (2013) 727–736. doi:10.1038/nrm3683.

[48] G. Zhu, X. Chen, X. Wang, X. Li, Q. Du, H. Hong, N. Tang, F. She, Y. Chen, Expression of the RIP-1 Gene and its Role in Growth and Invasion of Human Gallbladder Carcinoma, Cell. Physiol. Biochem. 34 (2014) 1152–1165. doi:10.1159/000366328.

[49] K.D. McCormick, A. Ghosh, S. Trivedi, L. Wang, C.B. Coyne, R.L. Ferris, S.N. Sarkar, Innate immune signaling through differential RIPK1 expression promote tumor progression in head and neck squamous cell carcinoma, Carcinogenesis. 37 (2016) 522–529. doi:10.1093/carcin/bgw032.

[50] M. Dajon, K. Iribarren, I. Cremer, Toll-like receptor stimulation in cancer: A pro- and anti-tumor double-edged sword, Immunobiology. 222 (2017) 89–100. doi:10.1016/j.imbio.2016.06.009.

[51] L. Friboulet, C. Pioche-Durieu, S. Rodriguez, A. Valent, S. Souquère, H. Ripoche, A. Khabir, S.W. Tsao, J. Bosq, K.W. Lo, P. Busson, Recurrent overexpression of c-IAP2 in EBV-associated nasopharyngeal carcinomas: critical role in resistance to Toll-like receptor 3-mediated apoptosis., Neoplasia. 10 (2008) 1183–94. http://www.ncbi.nlm.nih.gov/pubmed/18953427 (accessed February 18, 2019).

[52] T.-C. Chou, Drug Combination Studies and Their Synergy Quantification Using the Chou-Talalay Method, Cancer Res. 70 (2010) 440–446. doi:10.1158/0008-5472.CAN-09-1947.

[53] A. Oberst, C.P. Dillon, R. Weinlich, L.L. McCormick, P. Fitzgerald, C. Pop, R. Hakem, G.S. Salvesen, D.R. Green, Catalytic activity of the caspase-8–FLIPL complex inhibits RIPK3-dependent necrosis, Nature. 471 (2011) 363–367. doi:10.1038/nature09852.

[54] A.R. Bernardo, J.M. Cosgaya, A. Aranda, A.M. Jiménez-Lara, Synergy between RA and TLR3 promotes type I IFN-dependent apoptosis through upregulation of TRAIL pathway in breast cancer cells, Cell Death Dis. 4 (2013) e479–e479. doi:10.1038/cddis.2013.5.

[55] M. Tanabe, M. Kurita-Taniguchi, K. Takeuchi, M. Takeda, M. Ayata, H. Ogura, M. Matsumoto, T. Seya, Mechanism of up-regulation of human Toll-like receptor 3 secondary to infection of measles virus-attenuated strains, Biochem. Biophys. Res. Commun. 311 (2003) 39–48. doi:10.1016/J.BBRC.2003.09.159.

[56] S. González-Reyes, J.M. Fernández, L.O. González, A. Aguirre, A. Suárez, J.M. González, S. Escaff, F.J. Vizoso, Study of TLR3, TLR4, and TLR9 in prostate carcinomas and their association with biochemical recurrence, Cancer Immunol. Immunother. 60 (2011) 217–226. doi:10.1007/s00262-010-0931-0.

[57] W.-M. Hsu, C.-C. Huang, P.-Y. Wu, H. Lee, M.-C. Huang, M.-H. Tai, J.-H. Chuang, Toll-like receptor 3 expression inhibits cell invasion and migration and predicts a favorable prognosis in neuroblastoma, Cancer Lett. 336 (2013) 338–346. doi:10.1016/j.canlet.2013.03.024.

[58] M.-M. Yuan, Y.-Y. Xu, L. Chen, X.-Y. Li, J. Qin, Y. Shen, TLR3 expression correlates with apoptosis, proliferation and angiogenesis in hepatocellular carcinoma and predicts

prognosis, BMC Cancer. 15 (2015) 245. doi:10.1186/s12885-015-1262-5.

[59] M.A. Aznar, L. Planelles, M. Perez-Olivares, C. Molina, S. Garasa, I. Etxeberría, G. Perez, I. Rodriguez, E. Bolaños, P. Lopez-Casas, M.E. Rodriguez-Ruiz, J.L. Perez-Gracia, I. Marquez-Rodas, A. Teijeira, M. Quintero, I. Melero, Immunotherapeutic effects of intratumoral nanoplexed poly I:C, J. Immunother. Cancer. 7 (2019) 116. doi:10.1186/s40425-019-0568-2.

[60] N. Umemura, J. Zhu, Y.K. Mburu, A. Forero, P.N. Hsieh, R. Muthuswamy, P. Kalinski, R.L. Ferris, S.N. Sarkar, Defective NF- B Signaling in Metastatic Head and Neck Cancer Cells Leads to Enhanced Apoptosis by Double-Stranded RNA, Cancer Res. 72 (2012) 45–55. doi:10.1158/0008-5472.CAN-11-1484.

[61] S. Fulda, Promises and Challenges of Smac Mimetics as Cancer Therapeutics, Clin. Cancer Res. 21 (2015) 5030–5036. doi:10.1158/1078-0432.CCR-15-0365.

[62] G.-B. Koo, M.J. Morgan, D.-G. Lee, W.-J. Kim, J.-H. Yoon, J.S. Koo, S. Il Kim, S.J. Kim, M.K. Son, S.S. Hong, J.M.M. Levy, D.A. Pollyea, C.T. Jordan, P. Yan, D. Frankhouser, D. Nicolet, K. Maharry, G. Marcucci, K.S. Choi, H. Cho, A. Thorburn, Y.-S. Kim, Methylation-dependent loss of RIP3 expression in cancer represses programmed necrosis in response to chemotherapeutics., Cell Res. 25 (2015) 707–25. doi:10.1038/cr.2015.56.

[63] P. Geserick, J. Wang, R. Schilling, S. Horn, P.A. Harris, J. Bertin, P.J. Gough, M. Feoktistova, M. Leverkus, Absence of RIPK3 predicts necroptosis resistance in malignant melanoma., Cell Death Dis. 6 (2015) e1884. doi:10.1038/cddis.2015.240.

[64] A. Annibaldi, P. Meier, Checkpoints in TNF-Induced Cell Death: Implications in

Inflammation and Cancer., Trends Mol. Med. 24 (2018) 49–65. doi:10.1016/j.molmed.2017.11.002.

[65] Z. Zhan, X. Xie, H. Cao, X. Zhou, X.D. Zhang, H. Fan, Z. Liu, Autophagy facilitates TLR4- and TLR3-triggered migration and invasion of lung cancer cells through the promotion of TRAF6 ubiquitination, Autophagy. 10 (2014) 257–268. doi:10.4161/auto.27162.

[66] C.D. Fingas, B.R.A. Blechacz, R.L. Smoot, M.E. Guicciardi, J. Mott, S.F. Bronk, N.W. Werneburg, A.E. Sirica, G.J. Gores, A smac mimetic reduces TNF related apoptosis inducing ligand (TRAIL)-induced invasion and metastasis of cholangiocarcinoma cells., Hepatology. 52 (2010) 550–61. doi:10.1002/hep.23729.

[67] E. Varfolomeev, T. Goncharov, A. V. Fedorova, J.N. Dynek, K. Zobel, K. Deshayes, W.J. Fairbrother, D. Vucic, c-IAP1 and c-IAP2 Are Critical Mediators of Tumor Necrosis Factor α (TNFα)-induced NF-κB Activation, J. Biol. Chem. 283 (2008) 24295–24299. doi:10.1074/jbc.C800128200.

[68] M.J.M. Bertrand, S. Milutinovic, K.M. Dickson, W.C. Ho, A. Boudreault, J. Durkin, J.W. Gillard, J.B. Jaquith, S.J. Morris, P.A. Barker, cIAP1 and cIAP2 Facilitate Cancer Cell Survival by Functioning as E3 Ligases that Promote RIP1 Ubiquitination, Mol. Cell. 30 (2008) 689–700. doi:10.1016/J.MOLCEL.2008.05.014.

[69] P. Rattanasinganchan, K. Leelawat, S. Treepongkaruna, C. Tocharoentanaphol, S. Subwongcharoen, T. Suthiphongchai, R. Tohtong, Establishment and characterization of a cholangiocarcinoma cell line (RMCCA-1) from a Thai patient, World J. Gastroenterol. 12 (2006) 6500. doi:10.3748/wjg.v12.i40.6500.

A

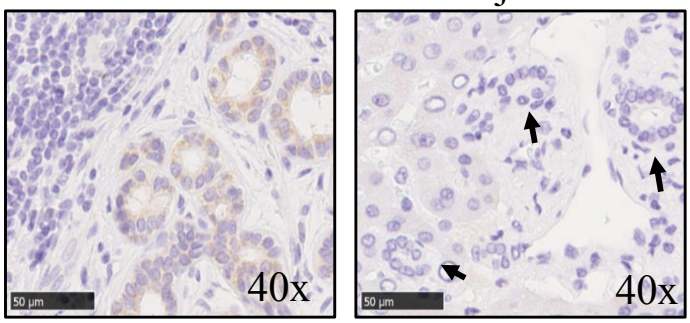


B

| Median of H-score | n | Area | | *p*-value |
|---|---|---|---|---|
| | | Tumor area | Tumor adjacent normal area | |
| All CCA | 88 | 78.09 (0-265) | 38.18 (0-100) | 2.248E-7 |
| Hilar | 67 | 86.49 (0-265) | 36.27 (0-100) | 2.837E-9 |
| Intrahepatic | 21 | 51.19 (0-240) | 44.29 (10-90) | 0.689 |

C

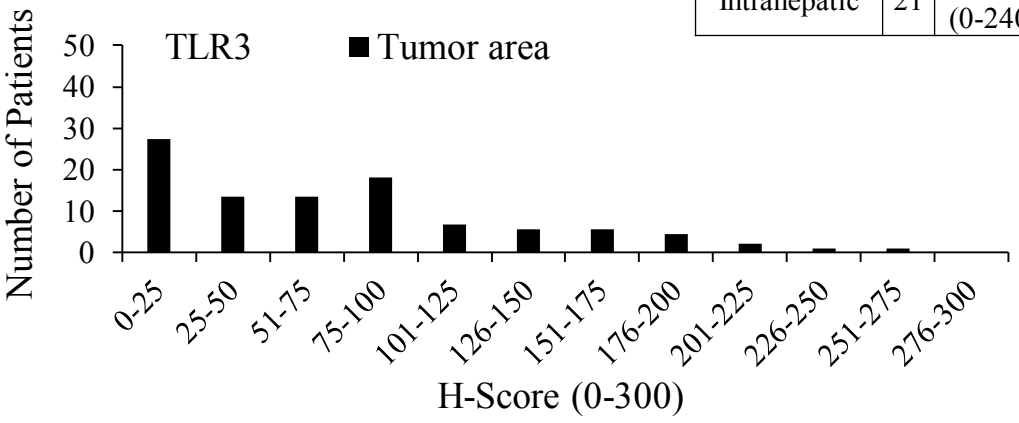


D

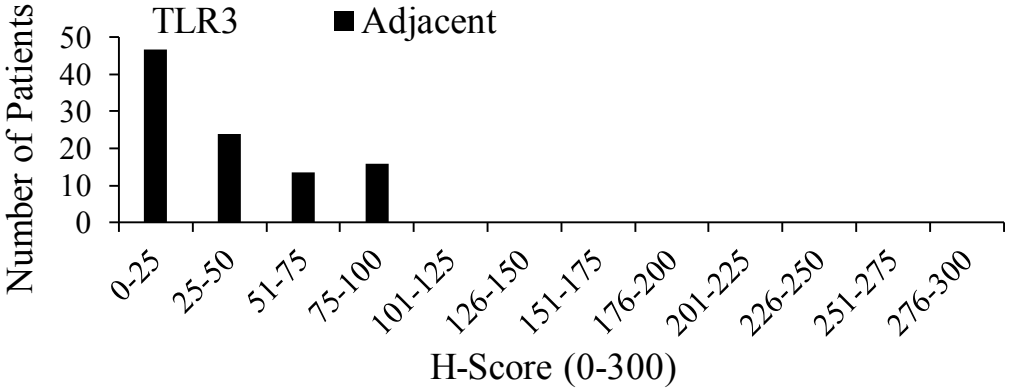


E

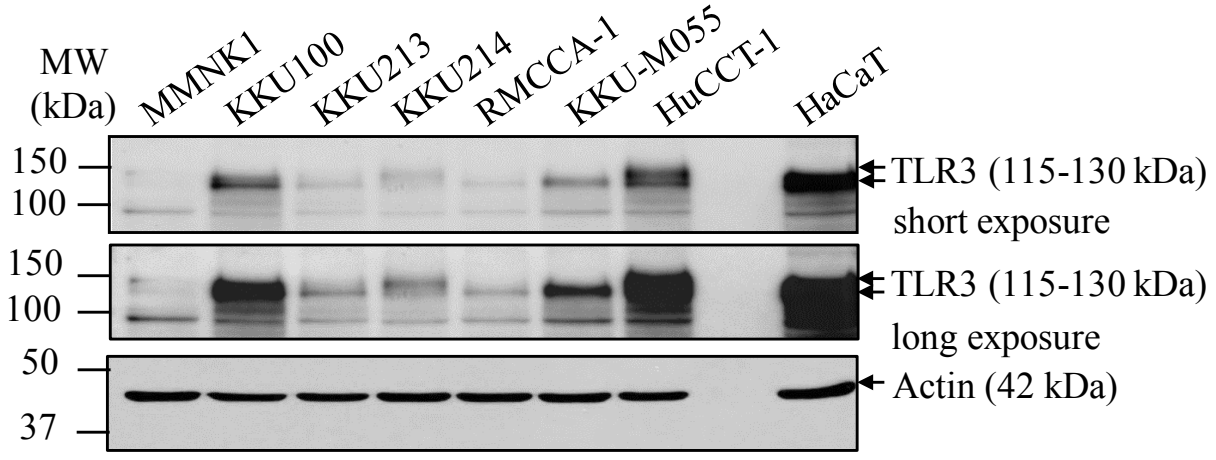


**Figure 1**

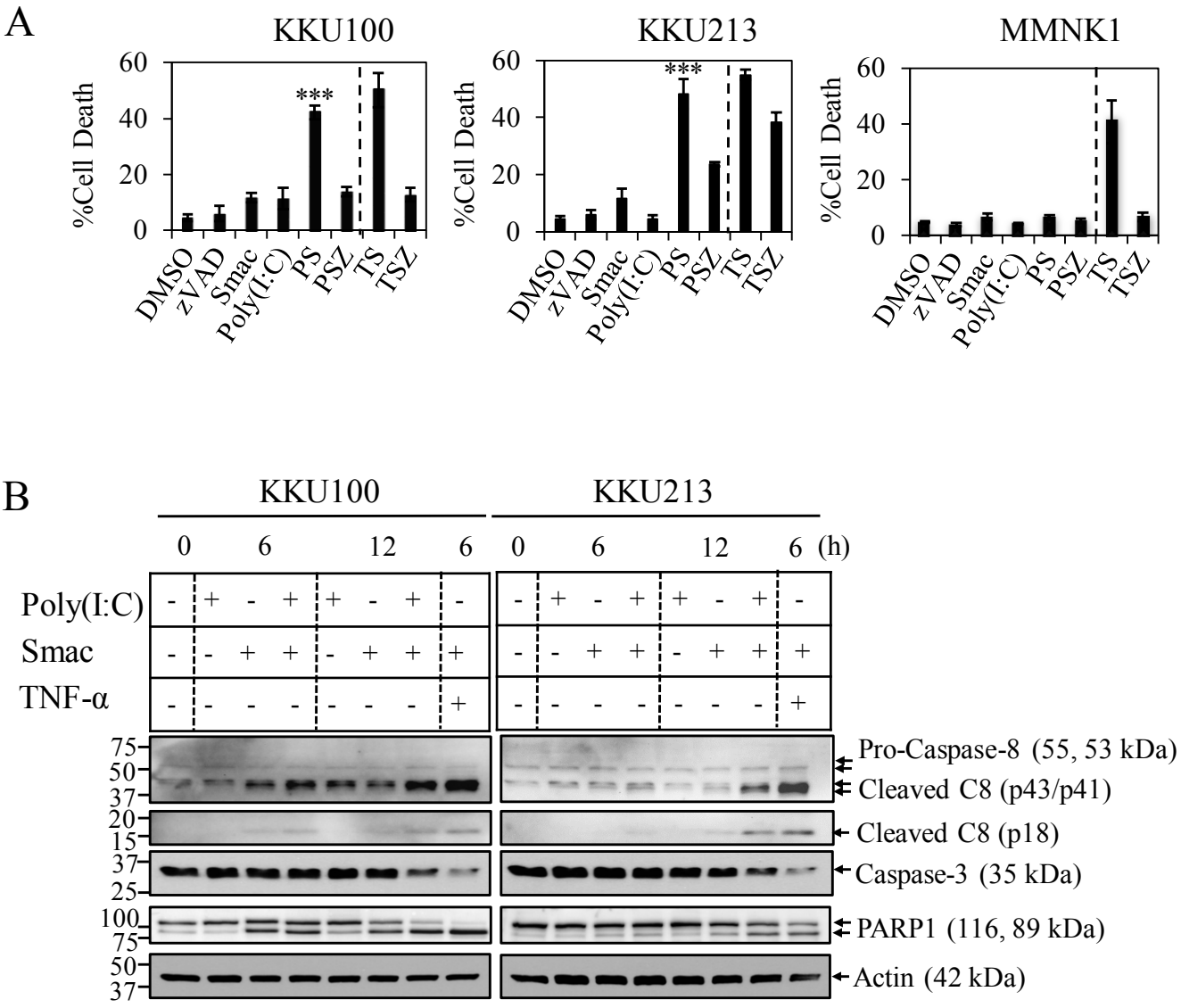
A
KKU100
KKU213
MMNK1
%Cell Death
60
40
20
0
***
DMSO
zVAD
Smac
Poly(I:C)
PS
PSZ
TS
TSZ
B
KKU100
KKU213
0
6
12
6
(h)
Poly(I:C)
Smac
TNF-α
75
50
37
20
15
25
100
Pro-Caspase-8 (55, 53 kDa)
Cleaved C8 (p43/p41)
Cleaved C8 (p18)
Caspase-3 (35 kDa)
PARP1 (116, 89 kDa)
Actin (42 kDa)

**Figure 2**

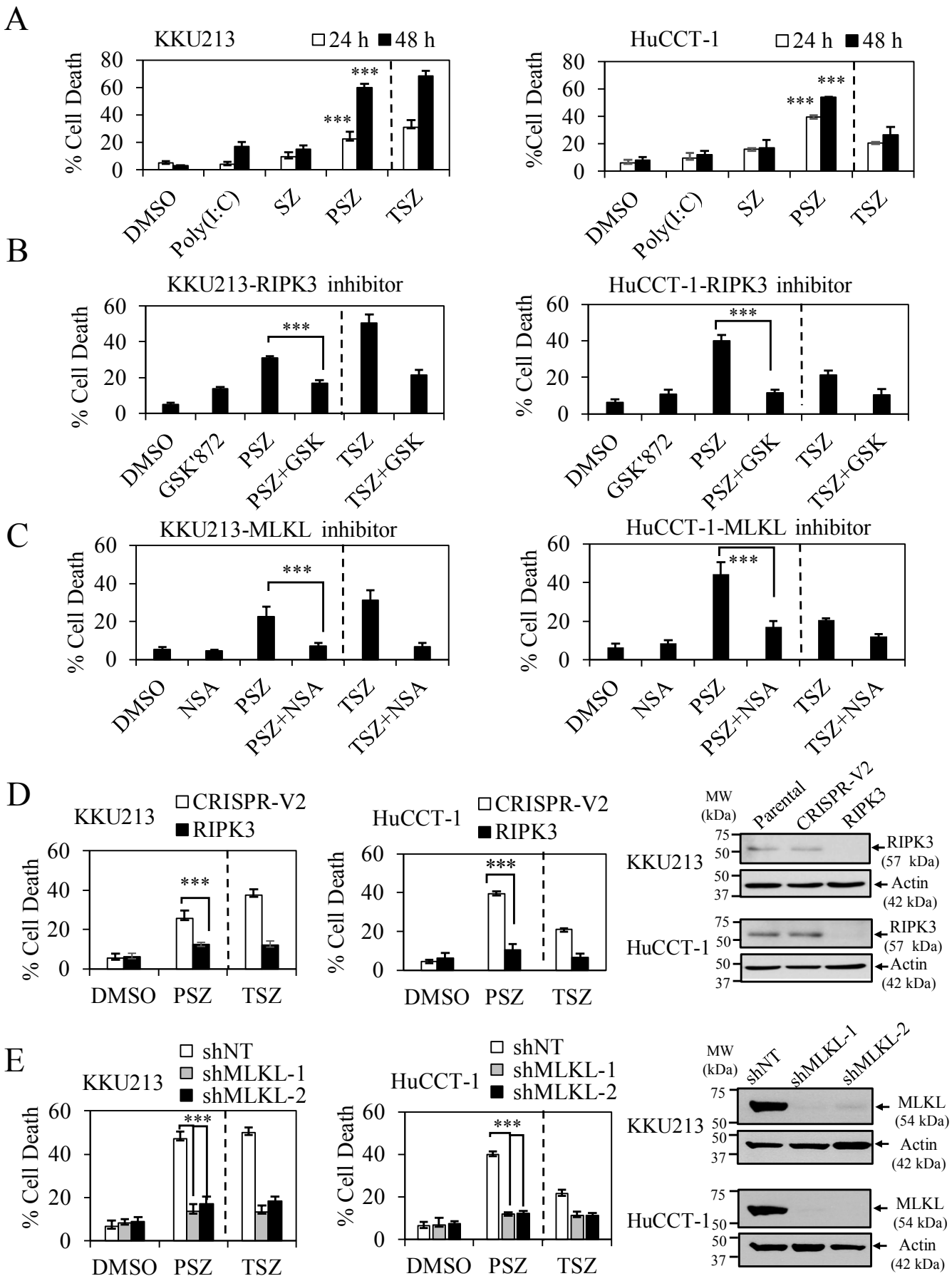
A
KKU213
24 h
48 h
% Cell Death
DMSO
Poly(I:C)
SZ
PSZ
TSZ
HuCCT-1
B
KKU213-RIPK3 inhibitor
HuCCT-1-RIPK3 inhibitor
GSK'872
PSZ+GSK
TSZ+GSK
C
KKU213-MLKL inhibitor
HuCCT-1-MLKL inhibitor
NSA
PSZ+NSA
TSZ+NSA
D
CRISPR-V2
RIPK3
MW (kDa)
Parental
CRISPR-V2
RIPK3
RIPK3 (57 kDa)
Actin (42 kDa)
E
shNT
shMLKL-1
shMLKL-2
MLKL (54 kDa)

**Figure 3**

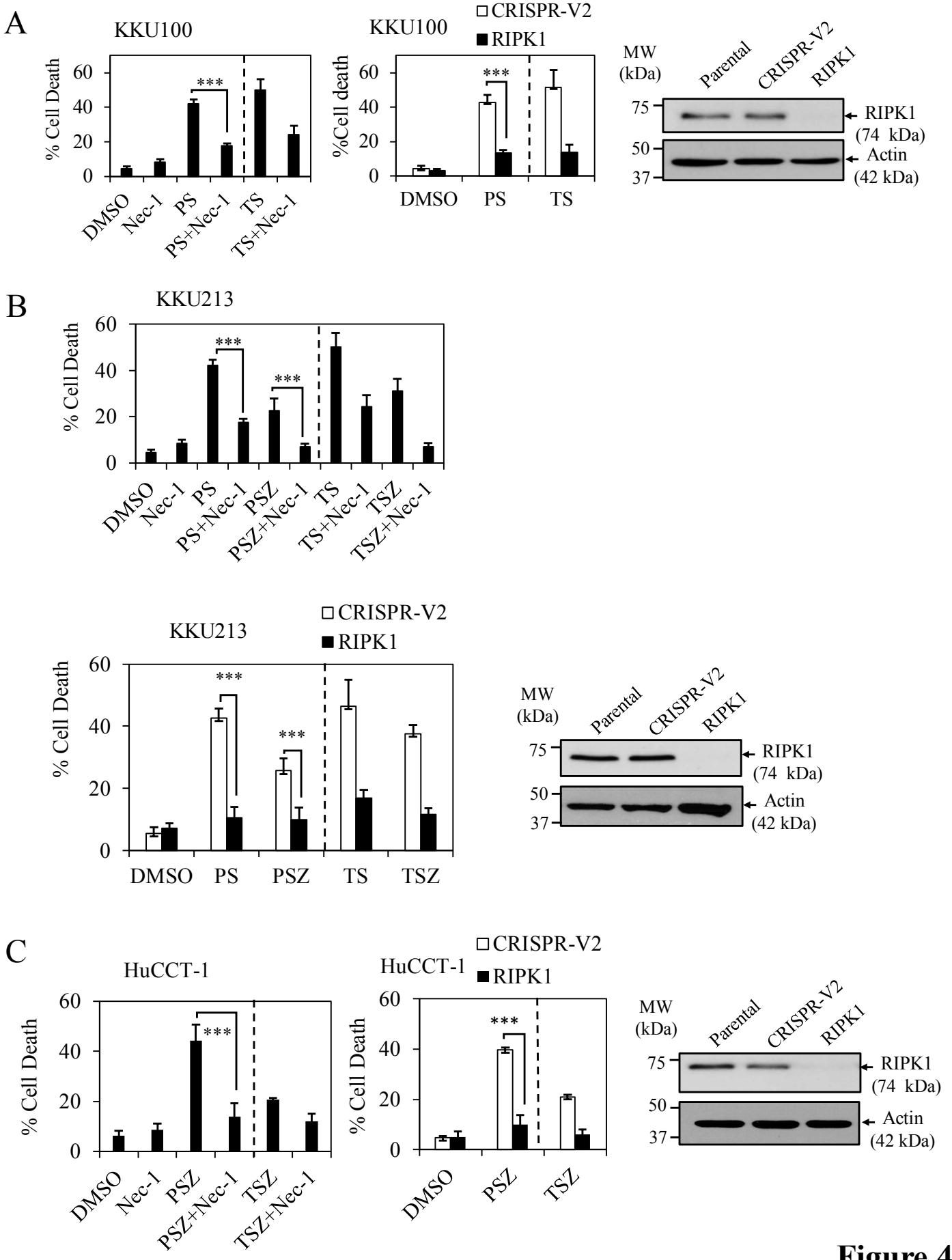
A
KKU100
% Cell Death
60
40
20
0
***
DMSO
Nec-1
PS
PS+Nec-1
TS
TS+Nec-1
KKU100
CRISPR-V2
RIPK1
%Cell death
DMSO
PS
TS
MW
(kDa)
Parental
CRISPR-V2
RIPK1
75
50
37
RIPK1
(74 kDa)
Actin
(42 kDa)
B
KKU213
PSZ
PSZ+Nec-1
TSZ
TSZ+Nec-1
C
HuCCT-1
PSZ
TSZ

**Figure 4**

A

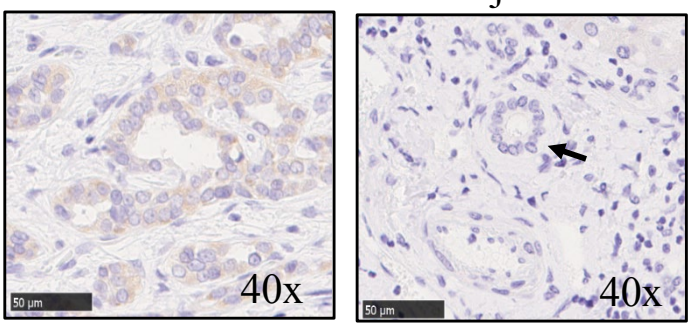


B

| Median of H-score | n | Area | | *p*-value |
|---|---|---|---|---|
| | | Tumor area | Tumor adjacent normal area | |
| All CCA | 88 | 39.20 (0-150) | 1.93 | 2.831E-18 |
| Hilar | 67 | 31.10 (0-110) | 2.39 | 1.303E-13 |
| Intrahepatic | 21 | 59.50 (0-150) | 1.77 | 3.739E-7 |
| Cholangiocytes | 8 | 11.25 | | |
| Liver cells | 8 | 61.25 | | |

C

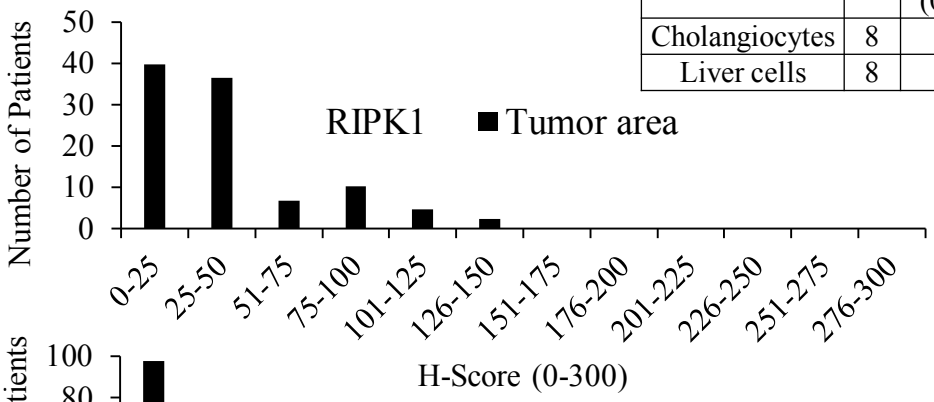


D

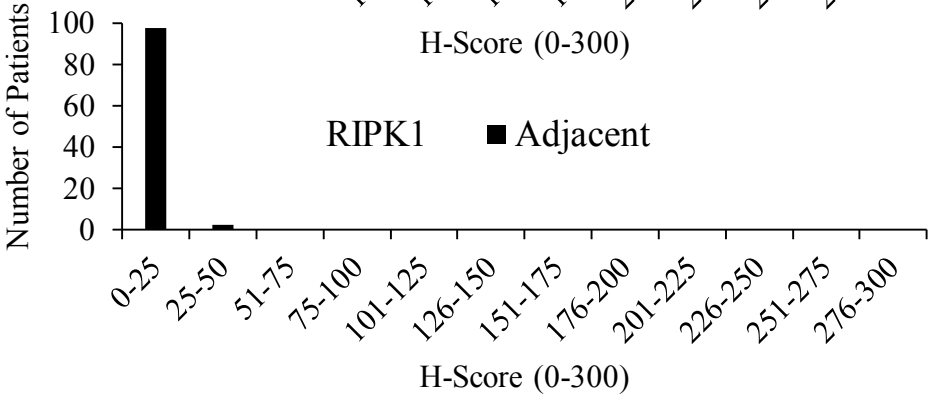


E

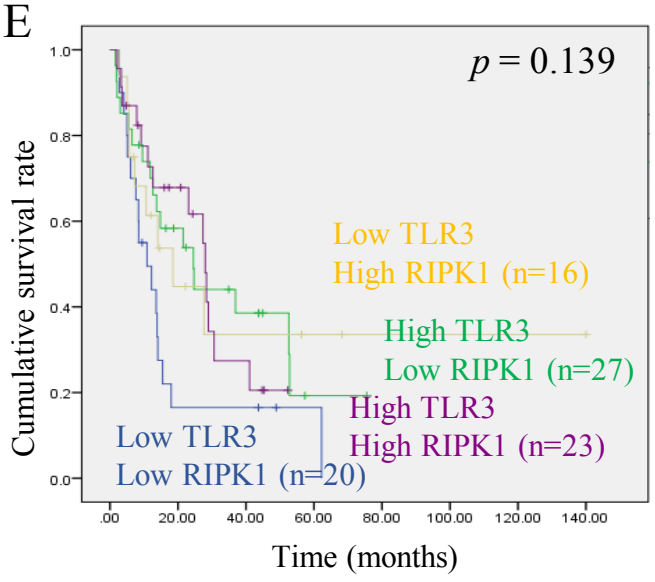


F

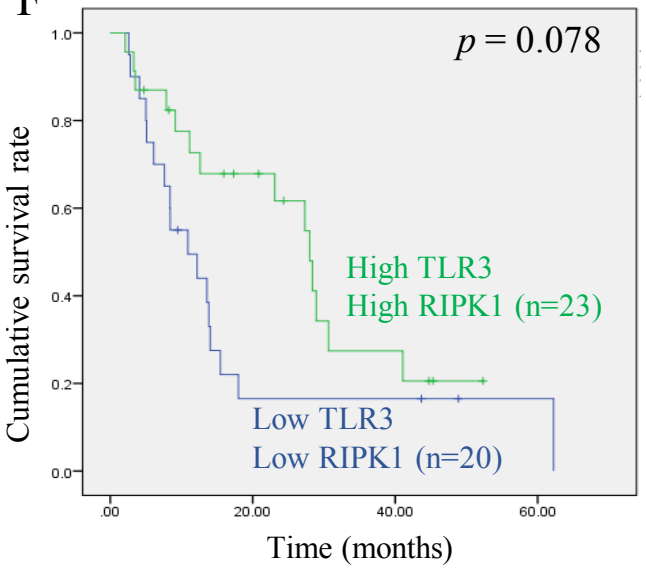


**Figure 5**

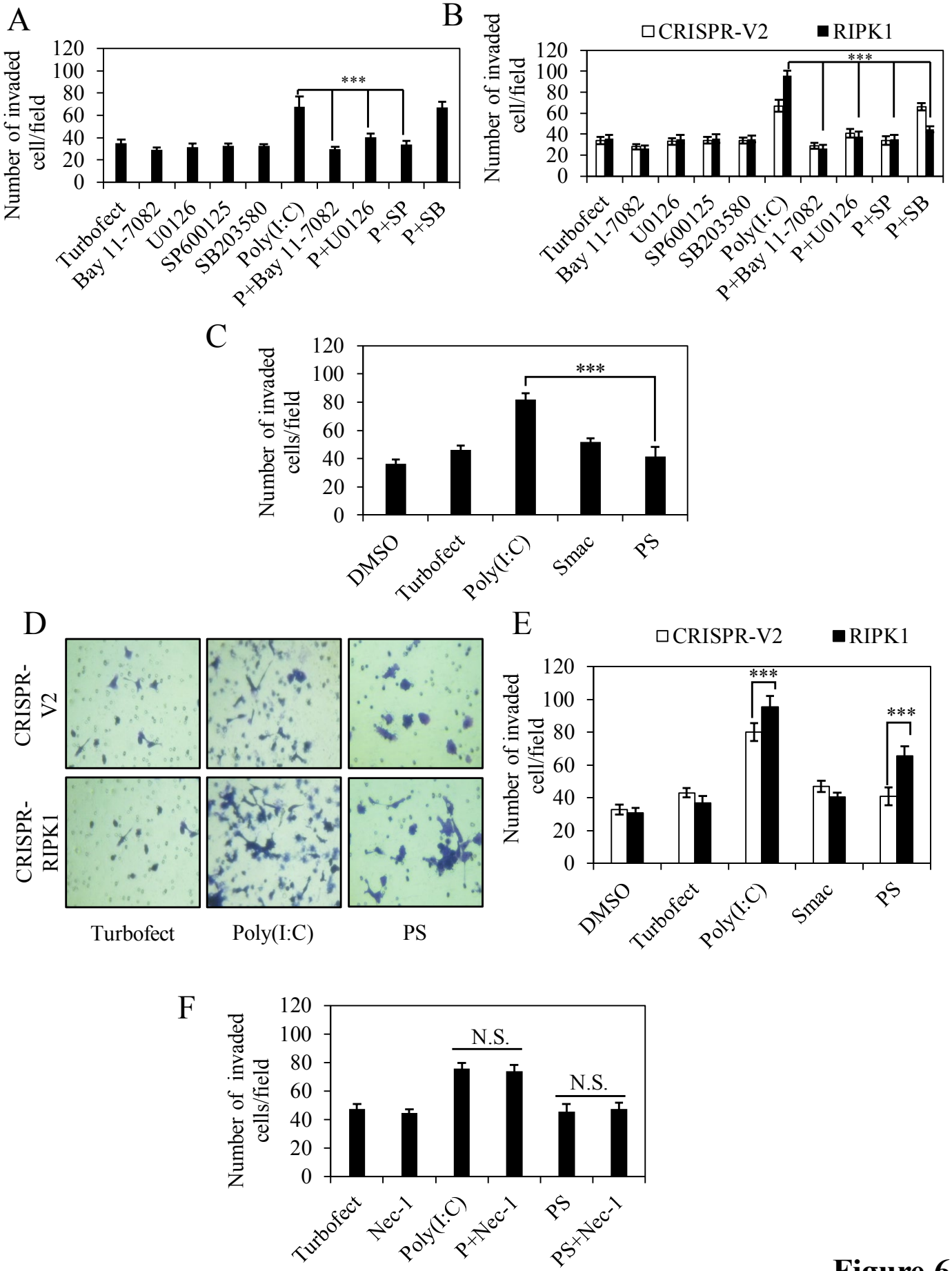
A
Number of invaded cell/field
120
100
80
60
40
20
0
***
Turbofect
Bay 11-7082
U0126
SP600125
SB203580
Poly(I:C)
P+Bay 11-7082
P+U0126
P+SP
P+SB
B
CRISPR-V2
RIPK1
Number of invaded cell/field
***
Turbofect
Bay 11-7082
U0126
SP600125
SB203580
Poly(I:C)
P+Bay 11-7082
P+U0126
P+SP
P+SB
C
Number of invaded cells/field
***
DMSO
Turbofect
Poly(I:C)
Smac
PS
D
CRISPR-V2
CRISPR-RIPK1
Turbofect
Poly(I:C)
PS
E
CRISPR-V2
RIPK1
Number of invaded cell/field
***
***
DMSO
Turbofect
Poly(I:C)
Smac
PS
F
Number of invaded cells/field
N.S.
N.S.
Turbofect
Nec-1
Poly(I:C)
P+Nec-1
PS
PS+Nec-1

**Figure 6**

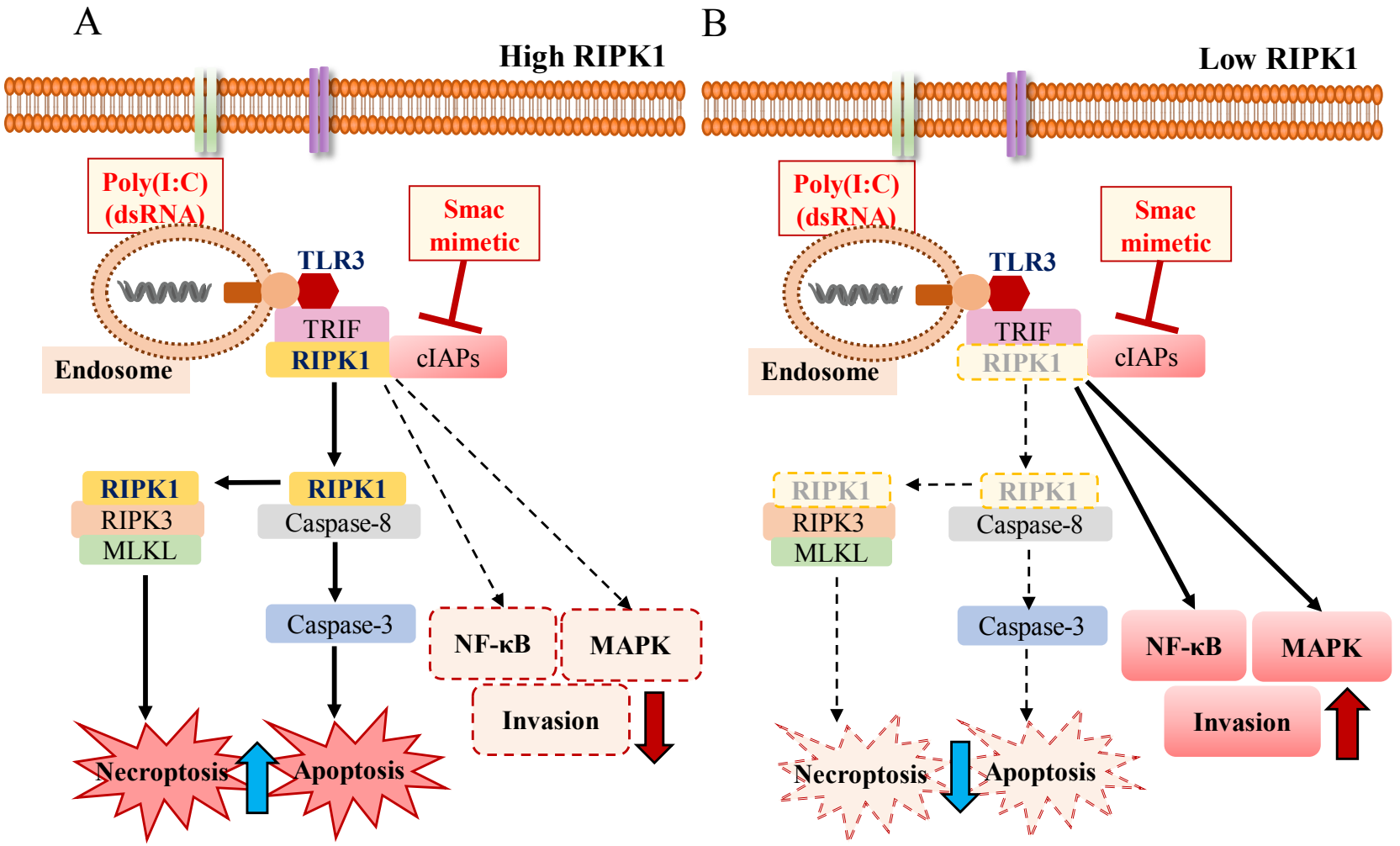
A
High RIPK1
Poly(I:C)
(dsRNA)
TLR3
TRIF
RIPK1
Endosome
Smac
mimetic
cIAPs
RIPK1
RIPK3
MLKL
RIPK1
Caspase-8
Caspase-3
NF-κB
MAPK
Invasion
Necroptosis
Apoptosis
B
Low RIPK1
Poly(I:C)
(dsRNA)
TLR3
TRIF
RIPK1
Endosome
Smac
mimetic
cIAPs
RIPK1
RIPK3
MLKL
RIPK1
Caspase-8
Caspase-3
NF-κB
MAPK
Invasion
Necroptosis
Apoptosis

**Figure 7**

| | | TLR3 | | Chi square | *p*-value | RIPK1 | | Chi square | *p*-value |
|---|---|---|---|---|---|---|---|---|---|
| **Gender** | n (%) | Low | High | | | Low | High | | |
| Male | 54 (39%) | 22 | 30 | 0.103 | 0.748 | 26 | 26 | 1.059 | 0.303 |
| Female | 35 (61%) | 14 | 22 | | | 22 | 14 | | |
| **Age (years)** | | | | | | | | | |
| < 67 | 44 (50%) | 19 | 25 | 0.188 | 0.665 | 28 | 16 | 2.933 | 0.087 |
| >= 67 | 44 (50%) | 17 | 27 | | | 20 | 24 | | |
| **Grading** | | | | | | | | | |
| well differentiated | 13 (14.8%) | 4 | 11 | 3.152 | 0.207 | 9 | 6 | 0.277 | 0.893 |
| moderately differentiated | 73 (83%) | 32 | 39 | | | 38 | 33 | | |
| poorly differentiated | 2 (2.2%) | 0 | 2 | | | 1 | 1 | | |
| **Tumor size (mm)** | | | | | | | | | |
| < 35 | 30 (38.5%) | 14 | 35 | 5.727 | **0.030** | 27 | 22 | 0.119 | 0.730 |
| >= 35 | 48 (61.5%) | 20 | 17 | | | 19 | 18 | | |
| **Perineural Invasion** | | | | | | | | | |
| Present | 65 (73%) | 22 | 43 | 5.132 | **0.023** | 43 | 22 | 13.517 | **0.0002** |
| None | 24 (27%) | 14 | 9 | | | 5 | 18 | | |
| **Vascular Invasion** | | | | | | | | | |
| Present | 66 (74.2%) | 21 | 45 | 9.026 | **0.003** | 41 | 25 | 6.111 | **0.013** |
| None | 23 (25.8%) | 15 | 7 | | | 7 | 15 | | |
| **Lymph node invasion** | | | | | | | | | |
| Present | 62 (69.7%) | 19 | 43 | 9.145 | **0.002** | 40 | 22 | 8.414 | **0.004** |
| None | 27 (30.3%) | 17 | 9 | | | 8 | 18 | | |

**Table 1**